Group-Based Approach to Derivatives of Delay Models Based on Incremental Queue Accumulations for Isolated Signalized Junctions

Seunghyeon Lee and S.C. Wong

Department of Civil Engineering, The University of Hong Kong, Pokfulam Road, Hong Kong, China

ABSTRACT

In this study, we devise an approximation method for the derivatives of group-based variables in individual signal groups during each cycle of a traffic signal, based on the estimated control delay formulas and queue formation patterns already defined by Lee and Wong (2017). Our goal is to establish the mathematical framework to compute the derivatives of the control delay under different traffic conditions on each cycle. The key challenges include establishing the most appropriate formulations to estimate the derivatives of the control delay toward group-based variables for individual lanes on each cycle, according to the queuing formation pattern, and identifying the vehicular arrivals and departures occurring in the extended or the setback time duration. We extract the group-based variables, including the start and the duration of the effective green time and the cycle time of each cycle, from the given signal plan to apply to the formulations of the lane-based control delay. The proposed methods are based on the formulations for the polygons on Incremental Queue Accumulations. We categorize the mathematical framework for the derivatives of the control delay in three cases based on the corresponding group of queuing formations defined by adjustment factors. The derivatives of the control delay computed by the proposed methods with respect to group-based variables are compared with numerical differentiations collected by simulation. The results of the two methods show good concurrence, with a few outliers for both the start and the duration of the effective green time. The proposed methods lay the foundation stone of more efficient and effective non-linear mathematical programs to optimize group-based signal plans with lane-based control delay as an objective function for each cycle for adaptive traffic control systems, both at isolated signalized junctions and in area traffic control.

Keywords: Incremental queue accumulations, Lane-based control delay, Adjustment factors, Group-based derivatives

1. INTRODUCTION

Traffic signals are the most effective way to deal with traffic flows that conflict with each other at isolated signalized junctions. Adaptive traffic control systems (ATCS) use signal timings created in real time based on the most up-to-date traffic detector information available. They have been installed in many metropolitan and suburban areas because they offer better performance than fixed-time and actuated controls, although the construction and operation costs are higher. To ensure that the control system can construct adaptive traffic control logics, it is important to estimate the control delay induced by queued vehicles over both the long and short term. Control delay is commonly used as a performance index in ATCS. The foundations of control delay studies were laid by Webster's theories and equations (Webster, 1958), stochastic queuing theory (Saaty, 1961), queued vehicular delay theory (Miller, 1963), and the time-dependent delay formula (Akçelik, 1980). The conservation equation (Lindley, 1952) and shockwave theory (Lighthill and Whitham, 1955; Richards, 1956) are the main queue estimation methods, and they are fundamental in integrating traditional

mathematical formulations for estimating control delay with the latest technologies for data collection and analysis. Diverse methods of estimating control delay have been developed, based on deterministic and stochastic approaches, since the establishment of these cornerstones of control delay and queue estimation methods. In addition, the cardinal concept of control delay, incremental queue accumulation (IQA), has been continuously developed in the U.S. Highway Capacity Manual (TRB, 2010) to improve its accuracy and robustness.

Due to its simplicity, the stage-based method has become the most common technique for constructing the pattern of signal timings at isolated signalized junctions and networks. It is based on a predetermined sequence of stages and inter-green periods. Mathematical programs to minimize delay and maximize capacity at a junction were introduced by Allsop (1971, 1972). Wong and Yang (1997, 1999) created stage-based optimization methods for network problems to minimize delay and maximize capacity, respectively. With the remarkable development of information technology for signal controllers in recent years, Heydecker and Dudgeon (1987) and Heydecker (1992) developed a group-based optimization method, in which signal settings are defined by the start and duration of green signal groups. This method can be used to overcome the limitations of the previous generation of signal optimization methods and has been used to develop more flexible signal structures applicable to a wider variety of urban traffic conditions and road layouts. The advantages of group-based optimization methods are achieved by simultaneously optimizing the structure of inter-green periods, cycle length, and signal sequence. Silcock (1997) specified a detailed mathematical framework for group-based optimization at isolated signalized junctions. Wong (1996, 1997) extended group-based methods to area traffic controls using derivatives of the performance index (Wong, 1995). A lane-based approach integrating the group-based optimization method with the geometric design of lane markings was established by Wong and Wong (2003a, 2003b) and Wong et al. (2006). A group-based method offers the advantages of more flexible signal plans for optimizing signal timings without affecting the cycle structure's predefined set of stages and signal sequence. To estimate the fluctuations in the vehicular delay caused by external factors, Wong (1995) devised derivatives of the performance index for the TRANSYT traffic model. For the fluctuation in the vehicular delay caused by external factors, Chow and Lo (2007) devised a derivative-based "GA+FW" to solve the cell-based signal control formulations; the approximated derivatives are comparable with numerical differentiation over long periods, but not at the cycle-by-cycle scale. Guler and Menendez (2014) derived the person delay in transportation systems that is caused by operating multi-modes of traffic flows at a signalized junction, including mixed-use lanes, dedicated bus lane, and PT priority signals.

In their introduction to the group-based method for ATCS, Lee et al. (2015b) considered the use of lane-to-lane turning flow estimation methods that are essential for constructing adaptive signal control logic in real time. The group-based variables, including the start and duration of the effective green time and the cycle time of each cycle, were extracted from the given signal plan and applied to formulations of the lane-based control delay. Lee et al. (2015a) developed a real-time estimation method for lane-based vertical queue lengths based on discriminant models and estimated downstream arrivals to estimate cycle delays for adaptive control logics. On the basis of estimated lane-based temporal and spatial data describing traffic flow conditions, a mathematical framework for estimating lane-based incremental queue accumulations (IQAs) was established by Lee and Wong (2017) using group-based variables and a predictive model for lane-based control delay. This established a rolling-horizon approach to lane-based control delay for group-based optimization of signal timings in ATCS.

Based on the abovementioned studies, group-based hierarchical adaptive traffic-signal control is proposed by Lee et al. (2017a, 2017b). The group-based formulation for adaptive signal-controls consists of a local reactive-control policy and a global proactive-optimization method. At the global level of control, a proactive global-optimization procedure is devised for group-based signal settings. Lee and Wong (2017) and the current study propose the estimation method of the total delay at the junction for a given signal plan and its derivatives, respectively. These estimates serve as the objective function and the gradient information for the formulation of a mathematical program. The group-based timing variables, that is, the start and duration of the green phase for each signal group, and the successor functions between conflicting signal groups are defined as the control variables in this mathematical program. The set of constraints includes limits on the duration of the green signal, clearance time, capacity, and various other constraints that govern the safety and operational requirements specified by the users. During the real-time operation of the current cycle, the queuing information is monitored by the real-time, second-by-second queue-length estimation procedure. The trigger switching occurs in the subsequent stage, when the criteria specified by the local control policy are met, or when the end of the transition zone time is reached. Therefore, the stage-switching time can occur before or after the time set by the global plan. The resolution of this local control level is in seconds, because changes to the signal features are decided second-by-second.

The present study outlines a method for approximating the derivatives of group-based variables of individual signal groups for each cycle, based on the estimated control delay formulas and already defined queue formation patterns. Partial differential equations of the IQA polygons for the group-based variables are used to estimate the derivatives. In addition to the derivatives, oversaturation components are used to analyze queuing formation patterns for each subsection of the lane-based IQAs. The proposed methods are major extensions of previous studies of the derivatives of vehicular delay and make the following three novel contributions: 1) real-time approximate expressions of derivatives that change cycle-by-cycle according to changing queuing formation patterns, 2) mathematical frameworks for derivatives of individual lanes, and 3) dynamically adapted mathematical frameworks for the most appropriate derivatives of the control delay of group-based variables for individual lanes for each cycle. The first contribution improves the temporal data, as the analysis time for the current real-time approximation methods is 60 s, which is not sufficient for calculating the robust values of traffic intensities that are needed to develop approximate expressions for derivatives. The second contribution improves the spatial data, as the previous approaches could not consider lane-changing behavior for lane-based queue lengths or the transient fluctuations of traffic flows at the micro level (second-by-second and cycle-by-cycle). For the third contribution, dynamic adapted mathematical frameworks, we formulate the lane-based control delay in every cycle as a combination of simple polygons in IQAs, which are defined by queue lengths at inflection points, adjustment factors, and group-based variables. These are similar to the parameters and variables used in the optimization process, and here they are used to develop an inexpensive computational mathematical framework to perform a cycle-by-cycle optimization process using the most up-to-date traffic information in real time.

The mathematical framework of the proposed methods is introduced in Section 2. The relevant contributions of previous studies, including the real-time method of estimating lane-based queue lengths and lane-based IQAs using group-based variables, are summarized in this section, and the derivatives of lane-based IQAs for each temporal section are then comprehensively described. To demonstrate the effectiveness of the developed equations, the results from these equations are compared with those from numerical differentiation in Section 3. The study's conclusions are given in Section 4.

2. METHODS

This section details the proposed method, including the group-based variables, and derivatives of the delay formula. The proposed data-processing method for the derivatives of lane-based IQAs is illustrated in Figure 1.

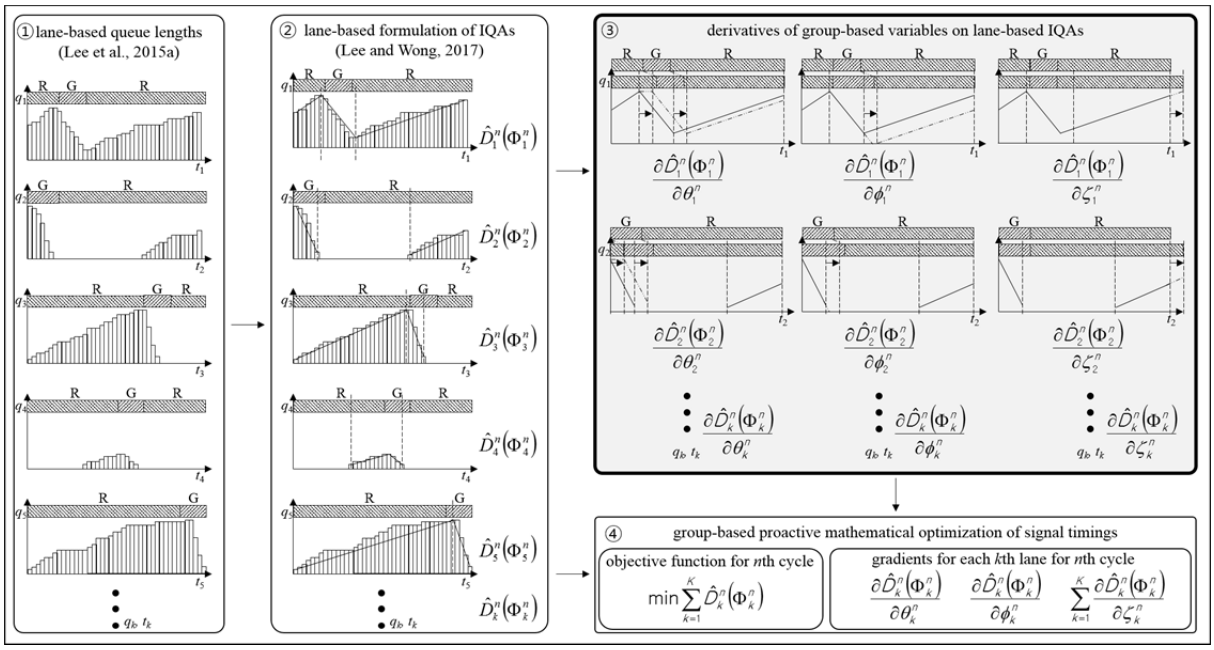

Figure 1. Data-processing method for derivatives of lane-based IQAs

In Figure 1.①, the temporal and spatial data describing real-time queue lengths in individual lanes are estimated using the method developed in Lee et al. (2015a). To formulate lane-based IQAs in real time, Figure 1.② follows Lee and Wong (2017) and specifies the polygons in the IQAs using group-based variables, including the start and duration of the green time for each signal group, a cycle time based on the estimated spatial and temporal coordinates, t_k, and the estimated queue lengths derived from Figure 1.①, q_k, for individual lanes. The aggregated control delay derived from the lane-based delay formula in Figure 1.②, $\hat{D}_k^n(\mathbf{\Phi}_k^n)$, is used as the objective function in the linear and non-linear mathematical programs used in the group-based proactive mathematical optimization of signal timings in Figure 1.④. Furthermore, the established formulation for control delay in Figure 1.② is used to construct the derivatives of the group-based variables for lane k in the nth cycle in Figure 1.③. The detailed mathematical framework for this process is presented in this study. In Figure 1.③, the partial differential equations of the polygons in the IQAs for specific group-based variable, θ_k^n, ϕ_k^n, and ζ^n, are used to estimate the derivatives. In addition, the oversaturation components are applied according to the queuing formation patterns defined by the adjustment factors in the three subsections of the control delay. These developed formulations are used as gradients to solve a non-convex function of group-based variables through a discrete directional search method for the group-based proactive mathematical optimization scheme in Figure 1.④. This data processing is performed every cycle in each lane to estimate the derivatives of the group-based variables in the established formulations for control delay. Definitions of the common indices, parameters, and variables used in this study are given below.

K	number of lanes
N	number of cycles
T	number of time steps in a cycle
$q_k^n(t)$	number of queued vehicles in lane k at time t in the nth cycle
θ_k^n	time from cycle origin to start of the actual green for control group k divided by cycle time in the nth cycle
ϕ_k^n	duration of the actual green for control group k divided by cycle time in the nth cycle
ζ^n	reciprocal value of cycle time in the nth cycle

K, N, and T are the common indices for the steps in this paper, and $q_k^n(t)$ represents the input data, which are the final output of the lane-based queue estimation models introduced by Lee et al. (2015a). θ_k^n, ϕ_k^n, and ζ^n are commonly used temporal group-based variables, as introduced by Heydecker and Dudgeon (1987).

2.1 Real-time method of estimating lane-based queue lengths

To deal with lane-changing behavior and counting errors, the modified conservation equation is given using estimated downstream arrivals, $\hat{a}_{\mathrm{d},k}^n(t)$, as

$$q_k^n(t) = \begin{cases} \max\left\{x_k^n(t) q_k^{n-1}(T) + \hat{a}_{\mathrm{d},k}^n(t) - i_{\mathrm{d},k}^n(t), 0\right\}, & \text{for } t = 1 \\ \max\left\{q_k^n(t-1) + \hat{a}_{\mathrm{d},k}^n(t) - i_{\mathrm{d},k}^n(t), 0\right\}. & \text{for } t \neq 1 \end{cases} \quad (1)$$

Lee et al. (2015a) have provided a detailed description of the overall process for estimating lane-based queue lengths. The number of queued vehicles in lane k at time t in the nth cycle, $q_k^n(t)$, is the maximum value between the conservation equation and zero to account for possible counting and passage errors. The first equation is used for the start time of each cycle, and the second for other time intervals. $q_k^{n-1}(T)$ is the number of queued vehicles in lane k at the last time point T in the ($n-1$)th cycle, and $x_k^n(t)$ is the output of the discriminant models. For example, if there is a residual queue in lane k at time T in the ($n-1$)th cycle, then $x_k^n(t)=1$, and otherwise it equals 0. Furthermore, let J be the set of upstream lanes, and K the set of downstream lanes. $i_{\mathrm{d},k}^n(t)$ is the downstream discharge according to the binary impulse memory from the downstream detector in lane k at time t in the nth cycle. The number of queued vehicles in each lane is recursively estimated on the basis of these equations in real time. These estimates are then used to establish a signal plan for the current cycle and calculate the stage-based pressure.

2.2 Lane-based IQAs using group-based variables

To explain their lane-based delay model, Lee and Wong (2017) specified polygons for the IQAs; the x- and y-coordinates of these polygons are based on spatial and temporal data on queue lengths, group-based variables, and adjustment factors collected from the previous step. The concept of lane-based IQAs using these variables is illustrated in Figure 2.

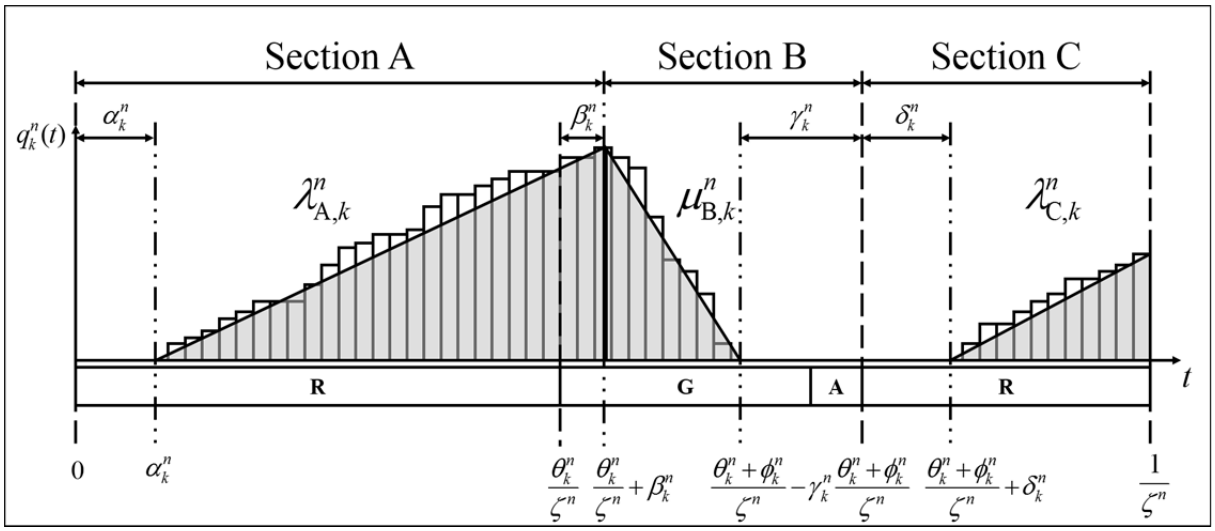

Figure 2. Lane-based incremental queue accumulations

In Figure 2, the y-coordinate is the queue length, and the x-coordinate is the time in seconds. The cycle time in the *n*th cycle is $1/\zeta^n$, and the start and end of the effective green time in lane *k* in the *n*th cycle are θ_k^n/ζ^n and $(\theta_k^n+\phi_k^n)/\zeta^n$, respectively. To improve the accuracy of the polygons in IQAs and identify queuing formation patterns in the current cycle, Lee and Wong (2017) introduced four adjustment factors for the temporal coordinate, α_k^n, β_k^n, γ_k^n, and δ_k^n. α_k^n accounts for the period when the queue length in lane *k* is zero during the red time before the effective green time in the *n*th cycle. Similarly, the period when the queue length in lane *k* is continuously increasing is captured by β_k^n, even if the current state of the signal controller is green in the *n*th cycle. γ_k^n accounts for the time slots during which lane *k* is empty during the effective green time in the *n*th cycle as a negative number, whereas γ_k^n becomes positive if the queue length is still discharging after the effective green time. The number of time units in which there are no queues in lane *k* during the red time after the effective green time in the *n*th cycle is described by δ_k^n. $\lambda_{A,k}^n$ and $\lambda_{C,k}^n$ are the arrival rates in lane *k* in the *n*th cycle in sections A and C, respectively. $\mu_{B,k}^n$ is the discharge rate in lane *k* in the *n*th cycle in section B. The arrival and discharge rates for individual lanes are calculated based on the spatial and temporal information obtained for queued vehicles.

For the total control delay formula in lane *k*, including all IQAs, the queuing formation patterns are classified into 24 cases based on the adjustment factors outlined in this study, rather than simply categorized as undersaturated or oversaturated traffic conditions. The queuing formation patterns during the red time before the effective green time are defined by α_k^n and β_k^n. In addition, the level of vehicular congestion during the effective green time is mainly captured by γ_k^n. δ_k^n describes the existence of residual queues during the red time after the effective green time. According to the value and sign of the factors, the mathematical formulations are differently applied for each lane during each cycle. The form of the total control delay in the *n*th cycle, including all adjustment factors, is given in Equation (2).

$$D^n = \frac{1}{2}\sum_{k=1}^{K}\left[\begin{array}{l}\left\{2\hat{q}_k^n\left(\alpha_k^n\right)+\lambda_{\mathrm{A},k}^n\left(\frac{\theta_k^n}{\zeta^n}+\beta_k^n-\alpha_k^n\right)\right\}\left(\frac{\theta_k^n}{\zeta^n}+\beta_k^n-\alpha_k^n\right)\\ +\left\{2\hat{q}_k^n\left(\alpha_k^n\right)+2\lambda_{\mathrm{A},k}^n\left(\frac{\theta_k^n}{\zeta^n}+\beta_k^n-\alpha_k^n\right)+\mu_{\mathrm{B},k}^n\left(\frac{\phi_k^n}{\zeta^n}+\gamma_k^n-\beta_k^n\right)\right\}\\ \left(\frac{\phi_k^n}{\zeta^n}+\gamma_k^n-\beta_k^n\right)+\left\{2\hat{q}_k^n\left(\frac{1}{\zeta^n}\right)-\lambda_{\mathrm{C},k}^n\left(\frac{1}{\zeta^n}-\frac{\theta_k^n+\phi_k^n}{\zeta^n}-\gamma_k^n-\delta_k^n\right)\right\}\\ \left(\frac{1}{\zeta^n}-\frac{\theta_k^n+\phi_k^n}{\zeta^n}-\gamma_k^n-\delta_k^n\right)\end{array}\right] \quad (2)$$

In Equation (2), the first part is the control delay in section A, which is related to a given trapezoid. The arrival rate during the red time before the effective green time, $\lambda_{\mathrm{A},k}^n$, is used to calculate the slope between two points, $\left(\alpha_k^n,\hat{q}_k^n\left(\alpha_k^n\right)\right),\left(\frac{\theta_k^n}{\zeta^n}+\beta_k^n,\hat{q}_k^n\left(\frac{\theta_k^n}{\zeta^n}+\beta_k^n\right)\right)$. The term in the first brace is the number of queued vehicles in lane *k* at α_k^n, $\hat{q}_k^n\left(\alpha_k^n\right)$, plus the number of queued vehicles in lane *k* at $\frac{\theta_k^n}{\zeta^n}+\beta_k^n$, $\hat{q}_k^n\left(\alpha_k^n\right)+\lambda_{\mathrm{A},k}^{\mathrm{n}}\left(\frac{\theta_k^n}{\zeta^n}+\beta_k^n-\alpha_k^n\right)$. The term in the second brace is the duration, $\frac{\theta_k^n}{\zeta^n}+\beta_k^n-\alpha_k^n$, during which the arrival rate is positive in section A.

The second part is for the control delay in section B. The discharge rate in lane *k* for the effective green time in the *n*th cycle, $\mu_{\mathrm{B},k}^n$, is given as a formula to calculate the slope between $\left(\frac{\theta_k^n}{\zeta^n}+\beta_k^n,\hat{q}_k^n\left(\frac{\theta_k^n}{\zeta^n}+\beta_k^n\right)\right)$ and $\left(\frac{\theta_k^n+\phi_k^n}{\zeta^n}+\gamma_k^n,\hat{q}_k^n\left(\frac{\theta_k^n+\phi_k^n}{\zeta^n}+\gamma_k^n\right)\right)$. The term in the first brace is the queue length in lane *k* at $\frac{\theta_k^n}{\zeta^n}+\beta_k^n$, $\hat{q}_k^n\left(\alpha_k^n\right)+\lambda_{\mathrm{A},k}^{\mathrm{n}}\left(\frac{\theta_k^n}{\zeta^n}+\beta_k^n-\alpha_k^n\right)$, plus the number of queued vehicles in lane *k* at $\frac{\theta_k^n+\phi_k^n}{\zeta^n}+\gamma_k^n$, $\hat{q}_k^n\left(\alpha_k^n\right)+\lambda_{\mathrm{A},k}^{\mathrm{n}}\left(\frac{\theta_k^n}{\zeta^n}+\beta_k^n-\alpha_k^n\right)+\mu_{\mathrm{B},k}^n\left(\frac{\phi_k^n}{\zeta^n}+\gamma_k^n-\beta_k^n\right)$. The term in the second brace is the duration, $\frac{\phi_k^n}{\zeta^n}+\gamma_k^n-\beta_k^n$, during which the discharge is negative in section B.

The last part describes the control delay in section C. The arrival rate in lane *k* for the effective green time in the *n*th cycle, $\lambda_{\mathrm{C},k}^n$, is given as a formula to calculate the slope between $\left(\frac{\theta_k^n+\phi_k^n}{\zeta^n}+\gamma_k^n+\delta_k^n,\hat{q}_k^n\left(\frac{\theta_k^n+\phi_k^n}{\zeta^n}+\gamma_k^n+\delta_k^n\right)\right)$ and $\left(\frac{1}{\zeta^n},\hat{q}_k^n\left(\frac{1}{\zeta^n}\right)\right)$. The term in the first brace is the number of queued vehicles in lane *k* at the temporal coordinate, expressed as $\frac{\theta_k^n+\phi_k^n}{\zeta^n}+\gamma_k^n+\delta_k^n$,

$\hat{q}_k^n\left(\frac{1}{\zeta^n}\right) - \lambda_{\mathrm{C},k}^n\left(\frac{1}{\zeta^n} - \frac{\theta_k^n + \phi_k^n}{\zeta^n} - \gamma_k^n - \delta_k^n\right)$, plus the number of queued vehicles in lane *k* at $\frac{1}{\zeta^n}$, $\hat{q}_k^n\left(\frac{1}{\zeta^n}\right)$. The term in the second brace is the duration, $\frac{1}{\zeta^n} - \frac{\theta_k^n + \phi_k^n}{\zeta^n} - \gamma_k^n - \delta_k^n$, during which the arrival rate is negative in section C.

To prevent abnormal fluctuation of the components, Equation (2) is transformed on the basis of four adjustment factors that describe traffic conditions during the *n*th cycle. Consequently, the formulation of the control delay is given by the following equation and sets of variables.

$$D^n = \frac{1}{2}\sum_{k=1}^{K}\left[D_{\mathrm{A},k}^n\left(\mathbf{\Gamma}^n, \mathbf{\Omega}_k^n, \mathbf{\Phi}_k^n\right) + D_{\mathrm{B},k}^n\left(\mathbf{\Gamma}^n, \mathbf{\Omega}_k^n, \mathbf{\Phi}_k^n\right) + D_{\mathrm{B},k}^n\left(\mathbf{\Gamma}^n, \mathbf{\Omega}_k^n, \mathbf{\Phi}_k^n\right)\right] \quad (3)$$

$$\mathbf{\Gamma}^n = \left\{\zeta^n, \theta_1^n \ldots \theta_k^n, \phi_1^n \ldots \theta_k^n\right\}, \forall k \in K, \forall n \in N$$

$$\mathbf{\Omega}_k^n = \left\{\alpha_k^n, \beta_k^n, \gamma_k^n, \delta_k^n\right\}, \forall k \in K, \forall n \in N$$

$$\Psi_k^n = \left\{\hat{q}_k^n\left(\alpha_k^n\right), \hat{q}_k^n\left(\frac{\theta_k^n}{\zeta^n} + \beta_k^n\right), \hat{q}_k^n\left(\frac{\theta_k^n + \phi_k^n}{\zeta^n} + \gamma_k^n\right), \hat{q}_k^n\left(\frac{\theta_k^n + \phi_k^n}{\zeta^n} + \gamma_k^n + \delta_k^n\right), \hat{q}_k^n\left(\frac{1}{\zeta^n}\right)\right\}$$

$$, \forall k \in K, \forall n \in N$$

$$\mathbf{\Phi}_k^n = \left\{\lambda_{\mathrm{A},k}^n, \mu_{\mathrm{B},k}^n, \lambda_{\mathrm{C},k}^n\right\}, \forall k \in K, \forall n \in N$$

Equation (3), with four sets of components, is identical to Equation (2). $\mathbf{\Gamma}^n$ is a set of group-based variables optimized on the basis of the predicted parameters in the optimization process for future study. $\mathbf{\Omega}_k^n$ is the set of adjustment factors used to decide the current state of queuing formation patterns in the current cycle. $\mathbf{\Psi}_k^n$ is the set of queue lengths at a given inflection point. $\mathbf{\Phi}_k^n$ is the set of slopes, including arrival rates before an effective green time, discharge rates, and arrival rates after an effective green time. Approximations are formulated for the derivatives of $\mathbf{\Gamma}^n$ based on $\mathbf{\Omega}_k^n$, $\mathbf{\Phi}_k^n$, and $\mathbf{\Psi}_k^n$ for the non-linear mathematical programs with the objective function, D^n.

2.3 Derivatives of lane-based IQAs

A small change in the specific group-based variable, including the start and duration of green time for each signal group, will influence the control delay based on lane-based polygons in the IQAs. The amount of change is quantified via the control delay induced by a one-second change in the group-based variable. The primary part of the formulation is derived from the partial differentiation of lane-based polygons in IQAs for each group. Moreover, the amount of temporal change in the control delay caused by vehicular arrivals for the extended and setback time durations is defined by an additional formula using temporal and spatial information on queue lengths for each section.

There are three distinct differences between the previous study in Lee and Wong (2017) and the proposed methods: 1) the approximate expressions for derivatives of the control delay formula, 2) adaptive systems that automatically select the most appropriate derivatives given the queue status in the current second and the group-based variables, and 3) the recognition that changes in each group-based variable under each specific queuing formation environment will result in changes in the control delay.

In the first contribution, the proposed methods provide a method for approximating the derivatives of group-based variables in individual signal groups during each cycle of a traffic signal, based on the estimated control delay formulas and queue formation patterns already defined by Lee et al. (2015a) and Lee and Wong (2017). Abridged descriptions of the previous studies, which are related to the proposed methods in this study, are provided in Sections 2.1 and 2.2. For the second contribution, the most suitable form of derivatives in sections A, B, and C are adaptively and automatically combined into the approximate expressions to produce an integrated derivative for each cycle for each individual lane. For section A, the derivatives for a specific group-based variable are automatically derived according to the values of alpha and beta and the existence of queued vehicles at the last time of section A. A change in the start of the effective green time exclusively determines the fluctuation in the control delay of section A, whereas the duration of the effective green time has no effect on the control delay of section A. For section B, approximate equations of derivatives are adaptively derived according to the value of beta, gamma, and delta and the existence of vehicles queues at each inflection point. The queue lengths at the first second of section B and the existence of residual vehicular queues after the end of the effective green time are significant issues for the analysis of the derivatives of the control delay with respect to the group-based variables in section B. For section C, a substantial change in the total control delay occurs in section C with respect to the group-based variables. The important criteria for deciding the form of the derivatives of the control delay in section C are the values of gamma and delta and the number of vehicular queues in which the arrival rate is positive after the effective green time. For the third contribution, the proposed methods can explain how a small change in group-based variables can influence the control delay based on the lane-based polygons in the IQAs for each temporal segment. The amount of change is quantified via the control delay induced by a one-second change in the group-based variables. The primary part of the formulation identifying this relationship derives from the partial differentiation of the lane-based polygons in the IQAs for each group. In addition to the influence of partial differentiation, the amount of temporal change in the control delay caused by vehicular arrivals for the extended and setback time durations is defined by an additional formula using temporal and spatial information on queue lengths for each section.

Derivatives of the control delay with respect to group-based control variables can be specified as

$$\frac{\partial D^n}{\partial \boldsymbol{\Gamma}^n} = \frac{1}{2}\sum_{k=1}^{K}\left[\frac{\partial D_{\mathrm{A},k}^n\left(\boldsymbol{\Gamma}^n,\boldsymbol{\Omega}_k^n,\boldsymbol{\Phi}_k^n\right)}{\partial \boldsymbol{\Gamma}^n}+\frac{\partial D_{\mathrm{B},k}^n\left(\boldsymbol{\Gamma}^n,\boldsymbol{\Omega}_k^n,\boldsymbol{\Phi}_k^n\right)}{\partial \boldsymbol{\Gamma}^n}+\frac{\partial D_{\mathrm{C},k}^n\left(\boldsymbol{\Gamma}^n,\boldsymbol{\Omega}_k^n,\boldsymbol{\Phi}_k^n\right)}{\partial \boldsymbol{\Gamma}^n}\right] \tag{4}$$

In Equation (4), the derivatives of the delay model essentially follow the forms of a partial differential equation of the lane-based polygons in IQAs consisting of the components introduced by Lee and Wong (2017). The first term represents the primary effect on the control delay in section A caused by a one-second change in the group-based variables. The second and third terms shows the influence of a small change in the group-based variables on the control delay in section B and section C, respectively.

2.3.1 *Section A*

For section A, the queuing formation patterns can be classified into four types according to the adjustment factors α_k^n and β_k^n. What distinguishes the four types is the existence of a queue at the start of the cycle and continuously increasing arrivals a few seconds after the start of the effective green time. Concerning derivatives, small changes in group-based variables have little effect on

changes in the total control delay regardless of the queuing formation patterns. In addition, a change in the *start* of the effective green time exclusively determines the fluctuation in the control delay of section A, whereas the *duration* of the effective green time has no effect on the control delay of section A. The change in control delay is portrayed in Figure 3.

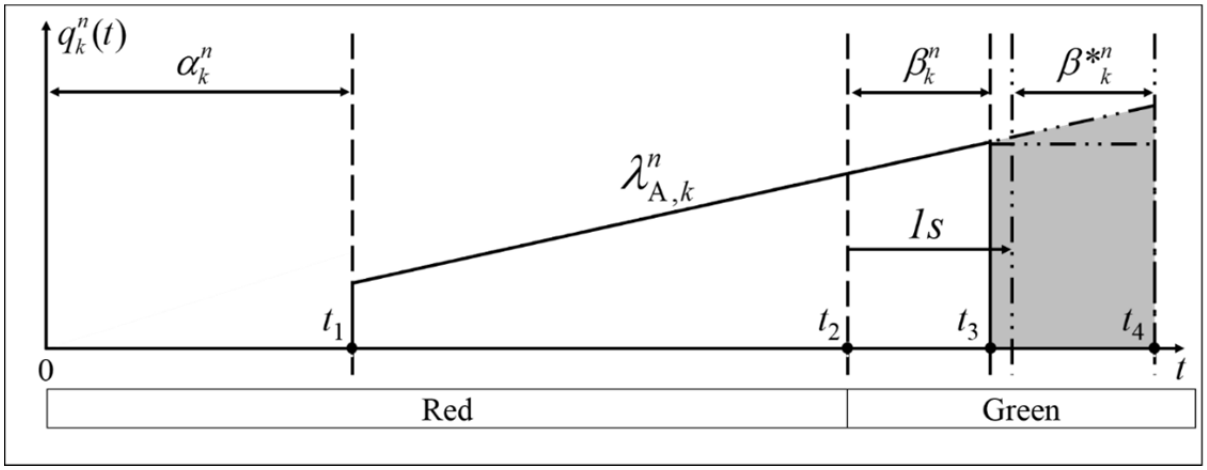

Figure 3. A change in the control delay in section A due to a small change in the group-based variables

In Figure 3, the control delay before and after a one-second change of the start of the effective green time is described by solid lines and two-dot chain lines, respectively. For the temporal information, t_1, t_2, t_3, and t_4 are α_k^n, $\frac{\theta_k^n}{\zeta^n}$, $\frac{\theta_k^n}{\zeta^n}+\beta_k^n$, and $\frac{\theta_k^n}{\zeta^n}+\beta_k^n+1$, respectively. β_k^n, the number of time slots in which the arrival rate is positive after the start of the effective green time, captures the existence of vehicles still queued after the start of the effective green time. If β_k^n is zero, the arrival rate during the red time before the effective green time, $\lambda^n_{A,k}$, will remain unchanged and the adjustment factors, α_k^n and β_k^n, will also be unaffected by the change in the start of the effective green time. In contrast, the arrival rate, $\lambda^n_{A,k}$, will be affected by a change in the start of the effective green time if β_k^n is larger than zero, due to a likely increase in queue lengths between $\frac{\theta_k^n}{\zeta^n}+\beta_k^n$ and $\frac{\theta_k^n}{\zeta^n}+\beta_k^n+1$. The change in the control delay and the additional increase are shown as the rectangle and small triangle around the two-dot chain lines on the highlighted area in Figure 3. Accordingly, the derivatives of the control delay with respect to group-based variables, Equations (7a), (7b), (8), and (9), can be obtained from Equations (5) and (6).

$$D^n_{A,k}=\frac{1}{2}\left[\left\{2\hat{q}_k^n\left(\alpha_k^n\right)+\lambda^n_{A,k}\left(\frac{\theta_k^n}{\zeta^n}+\beta_k^n-\alpha_k^n\right)\right\}\left(\frac{\theta_k^n}{\zeta^n}+\beta_k^n-\alpha_k^n\right)\right] \tag{5}$$

$$\lambda^n_{A,k}=\frac{\hat{q}_k^n\left(\frac{\theta_k^n}{\zeta^n}+\beta_k^n\right)-\hat{q}_k^n\left(\alpha_k^n\right)}{\frac{\theta_k^n}{\zeta^n}+\beta_k^n-\alpha_k^n} \tag{6}$$

$$\frac{\partial D_{\mathrm{A},k}^{n}}{\partial \theta_{k}^{n}} = \hat{q}_{k}^{n}\left(\alpha_{k}^{n}\right) + \lambda_{\mathrm{A},k}^{n}\left(\frac{\theta_{k}^{n}}{\zeta^{n}} + \beta_{k}^{n} - \alpha_{k}^{n}\right), \text{ If } \beta_{k}^{n} = 0. \tag{7a}$$

$$\frac{\partial D_{\mathrm{A},k}^{n}}{\partial \theta_{k}^{n}} = \hat{q}_{k}^{n}\left(\alpha_{k}^{n}\right) + \lambda_{\mathrm{A},k}^{n}\left(\frac{\theta_{k}^{n}}{\zeta^{n}} + \beta_{k}^{n} - \alpha_{k}^{n}\right) + 0.5, \text{ If } \beta_{k}^{n} > 0. \tag{7b}$$

$$\frac{\partial D_{\mathrm{A},k}^{n}}{\partial \phi_{k}^{n}} = 0 \tag{8}$$

$$\frac{\partial D_{\mathrm{A},k}^{n}}{\partial \zeta^{n}} = -\frac{1}{\left(\zeta^{n}\right)^{2}}\left\{\hat{q}_{k}^{n}\left(\alpha_{k}^{n}\right) + \lambda_{\mathrm{A},k}^{n}\left(\frac{\theta_{k}^{n}}{\zeta^{n}} + \beta_{k}^{n} - \alpha_{k}^{n}\right)\right\}\theta_{k}^{n} \tag{9}$$

The arrival rate and control delay in section A are computed by Equations (5) and (6). In Equation (7a), if β_{k}^{n} is zero, the control delay in section A, in the form of nonlinear partial differential equations, is partially differentiated for the start of the effective green time, θ_{k}^{n}. In Equation (7b), if β_{k}^{n} is larger than 0, the control delay in section A consists of the partially differentiated equation and the area of the shaded triangle in Figure 3. If the vehicle arrives between $\frac{\theta_{k}^{n}}{\zeta^{n}} + \beta_{k}^{n}$ and $\frac{\theta_{k}^{n}}{\zeta^{n}} + \beta_{k}^{n} + 1$, the increase in the queue lengths is one vehicle regardless of the arrival rate, $\lambda_{\mathrm{A},k}^{n}$, and the area of the shaded triangle becomes 0.5. The derivative of the control delay in section A for the duration of the effective green time, ϕ_{k}^{n}, is zero in Equation (8). The derivative of the control delay for the reciprocal of the cycle time is expressed by Equation (9).

2.3.2 *Section B*

For section B, the queuing formation patterns can be categorized into six types according to the adjustment factors β_{k}^{n} and γ_{k}^{n}. β_{k}^{n} is the number of seconds in which the arrival rate is positive during the effective green time. γ_{k}^{n} is the adjustment factor for the end of the effective green time. γ_{k}^{n} is the number of time units with a negative sign during which lane *k* is empty during the effective green time. If the discharge rate is negative during the red periods after the effective green time, γ_{k}^{n} is set as the number of seconds until discharge stops after the effective green time in the *n*th cycle; otherwise, γ_{k}^{n} is set as zero. The queue lengths at the last second of section A and the existence of residual queues after the end of the effective green time are key issues for the analysis of the derivatives of the control delay with respect to group-based variables in section B. Changes in the control delay for section B due to minor changes in the group-based variables are insignificant relative to the change in the total control delay. The control delay fluctuates due to changes in both the start and duration of the effective green time in section B; a diagram of a change in the control delay is given in Figure 4.

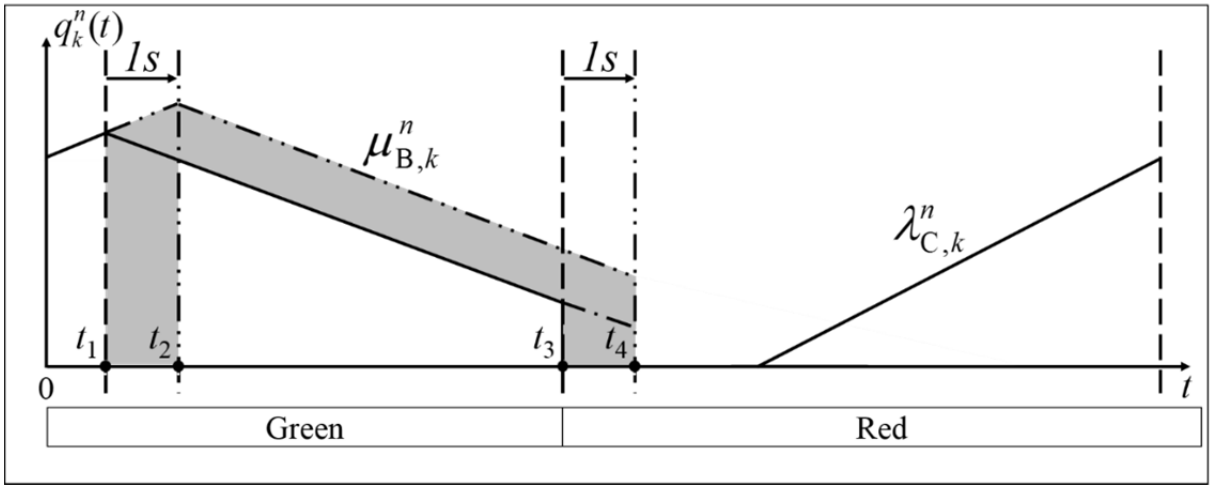

Figure 4. A change in the control delay in section B due to a small change in the group-based variables

In Figure 4, the original control delay is indicated by solid lines, whereas the shaded parts of the control delay, caused by changes in the start and duration of the effective green time, are shown by two-dot and one-dot chain lines, respectively. For the temporal information, t_1, t_2, t_3, and t_4 are $\frac{\theta_k^n}{\zeta^n}+\beta_k^n$, $\frac{\theta_k^n}{\zeta^n}+\beta_k^n+1$, $\frac{\theta_k^n+\phi_k^n}{\zeta^n}+\gamma_k^n$, and $\frac{\theta_k^n+\phi_k^n}{\zeta^n}+\gamma^*{}_k^n+1$, respectively. $\gamma^*{}_k^n$ is the changed version of the adjustment factor γ_k^n, due to minor changes in the group-based variables. The discharge rate in lane k on the nth cycle, $\mu_{\mathrm{B},k}^n$, remains unaffected by changes in the group-based variables, while the adjustment factor, γ_k^n, is affected by changes in the variables according to the temporal position of the end of a discharge.

For the start of the effective green time, the queue lengths at $\frac{\theta_k^n}{\zeta^n}+\beta_k^n+1$ are determined for section A by the derivatives in Equations (6.7a) and (6.7b), which give the change in the start of the effective green time. In addition, the number of queued vehicles at $\frac{\theta_k^n+\phi_k^n}{\zeta^n}+\gamma^*{}_k^n+1$ is calculated using $\mu_{\mathrm{B},k}^n$, $q_k^n\left(\frac{\theta_k^n}{\zeta^n}+\beta_k^n+1\right)$, and the period between $\frac{\theta_k^n}{\zeta^n}+\beta_k^n+1$ and $\frac{\theta_k^n+\phi_k^n}{\zeta^n}+\gamma^*{}_k^n+1$.

For the duration of the effective green time, the amount of change in the control delay is smaller than that induced by the start of the effective green time. If the queue lengths at $\frac{\theta_k^n+\phi_k^n}{\zeta^n}+\gamma_k^n$ are zero, the derivatives of the control delay caused by the duration of the effective green time are also zero; otherwise, the derivatives of the control delay are created from the partial differentiation of the control delay in section B. Accordingly, the derivatives of the control delay with respect to the group-based variables, Equations (12a), (12b), (12c), (12d), (13), and (14), can be obtained from Equations (10) and (11).

$$\mu_{\mathrm{B},k}^{n}=\frac{\hat{q}_{k}^{n}\left(\frac{\theta_{k}^{n}+\phi_{k}^{n}}{\zeta^{n}}+\gamma_{k}^{n}\right)-\hat{q}_{k}^{n}\left(\frac{\theta_{k}^{n}}{\zeta^{n}}+\beta_{k}^{n}\right)}{\frac{\phi_{k}^{n}}{\zeta^{n}}+\gamma_{k}^{n}-\beta_{k}^{n}} \tag{10}$$

$$D_{\mathrm{B},k}^{n}=\frac{1}{2}\left\{\begin{array}{l}2\hat{q}_{k}^{n}\left(\alpha_{k}^{n}\right)+2\lambda_{\mathrm{A},k}^{n}\left(\frac{\theta_{k}^{n}}{\zeta^{n}}+\beta_{k}^{n}-\alpha_{k}^{n}\right)\\+\mu_{\mathrm{B},k}^{n}\left(\frac{\phi_{k}^{n}}{\zeta^{n}}+\gamma_{k}^{n}-\beta_{k}^{n}\right)\end{array}\right\}\left(\frac{\phi_{k}^{n}}{\zeta^{n}}+\gamma_{k}^{n}-\beta_{k}^{n}\right) \tag{11}$$

If $\beta_{k}^{n}=0$ and $\gamma_{k}^{n}\leq -3$,

$$D*_{\mathrm{B},k}^{n}=\frac{1}{2}\left\{2\hat{q}_{k}^{n}\left(\alpha_{k}^{n}\right)+2\lambda_{\mathrm{A},k}^{n}\left(\frac{\theta_{k}^{n}}{\zeta^{n}}+\beta_{k}^{n}-\alpha_{k}^{n}\right)+\mu_{\mathrm{B},k}^{n}\left(\frac{\phi_{k}^{n}}{\zeta^{n}}+\gamma_{k}^{n}-\beta_{k}^{n}\right)\right\}\left(\frac{\phi_{k}^{n}}{\zeta^{n}}+\gamma_{k}^{n}-\beta_{k}^{n}\right)$$

$$\frac{\partial D_{\mathrm{B},k}^{n}}{\partial\theta_{k}^{n}}=D*_{\mathrm{B},k}^{n}-D_{\mathrm{B},k}^{n}=0 \tag{12a}$$

If $\beta_{k}^{n}=0$ and $\gamma_{k}^{n}>-3$

$$D*_{\mathrm{B},k}^{n}=\frac{1}{2}\left\{\begin{array}{l}2\hat{q}_{k}^{n}\left(\alpha_{k}^{n}\right)+2\lambda_{\mathrm{A},k}^{n}\left(\frac{\theta_{k}^{n}}{\zeta^{n}}+\beta_{k}^{n}-\alpha_{k}^{n}\right)\\+\mu_{\mathrm{B},k}^{n}\left(\frac{\phi_{k}^{n}}{\zeta^{n}}+\gamma_{k}^{n}-\beta_{k}^{n}-1\right)\end{array}\right\}\left(\frac{\phi_{k}^{n}}{\zeta^{n}}+\gamma_{k}^{n}-\beta_{k}^{n}-1\right)$$

$$\frac{\partial D_{\mathrm{B},k}^{n}}{\partial\theta_{k}^{n}}=\frac{1}{2}\left\{\begin{array}{l}\mu_{\mathrm{B},k}^{n}-2\hat{q}_{k}^{n}\left(\alpha_{k}^{n}\right)-2\lambda_{\mathrm{A},k}^{n}\left(\frac{\theta_{k}^{n}}{\zeta^{n}}+\beta_{k}^{n}-\alpha_{k}^{n}\right)\left(\frac{\phi_{k}^{n}}{\zeta^{n}}+\gamma_{k}^{n}-\beta_{k}^{n}\right)\\-2\mu_{\mathrm{B},k}^{n}\left(\frac{\phi_{k}^{n}}{\zeta^{n}}+\gamma_{k}^{n}-\beta_{k}^{n}\right)\end{array}\right\} \tag{12b}$$

If $\beta_{k}^{n}>0$ and $\gamma_{k}^{n}\leq -3$,

$$D*_{\mathrm{B},k}^{n}=\frac{1}{2}\left[\begin{array}{l}2\hat{q}_{k}^{n}\left(\alpha_{k}^{n}\right)+2\left\{\lambda_{\mathrm{A},k}^{n}\left(\frac{\theta_{k}^{n}}{\zeta^{n}}+\beta_{k}^{n}-\alpha_{k}^{n}\right)+0.5\right\}\\+\mu_{\mathrm{B},k}^{n}\left(\frac{\phi_{k}^{n}}{\zeta^{n}}+\gamma_{k}^{n}-\beta_{k}^{n}\right)\end{array}\right]\left(\frac{\phi_{k}^{n}}{\zeta^{n}}+\gamma_{k}^{n}-\beta_{k}^{n}\right)$$

$$\frac{\partial D_{\mathrm{B},k}^{n}}{\partial\theta_{k}^{n}}=\frac{1}{2}\left(\frac{\phi_{k}^{n}}{\zeta^{n}}+\gamma_{k}^{n}-\beta_{k}^{n}\right) \tag{12c}$$

If $\beta_{k}^{n}>0$ and $\gamma_{k}^{n}>-3$,

$$D*^{n}_{\mathrm{B},k} = \frac{1}{2}\left[\begin{array}{l} 2\hat{q}^{n}_{k}\left(\alpha^{n}_{k}\right)+2\left\{\lambda^{n}_{\mathrm{A},k}\left(\frac{\theta^{n}_{k}}{\zeta^{n}}+\beta^{n}_{k}-\alpha^{n}_{k}\right)+0.5\right\} \\ +\mu^{n}_{\mathrm{B},k}\left(\frac{\phi^{n}_{k}}{\zeta^{n}}+\gamma^{n}_{k}-\beta^{n}_{k}-1\right)\end{array}\right]\left(\frac{\phi^{n}_{k}}{\zeta^{n}}+\gamma^{n}_{k}-\beta^{n}_{k}-1\right)$$

$$\frac{\partial D^{n}_{\mathrm{B},k}}{\partial \theta^{n}_{k}} = \frac{1}{2}\left\{\begin{array}{l} \mu^{n}_{\mathrm{B},k}-2\hat{q}^{n}_{k}\left(\alpha^{n}_{k}\right)-2\lambda^{n}_{\mathrm{A},k}\left(\frac{\theta^{n}_{k}}{\zeta^{n}}+\beta^{n}_{k}-\alpha^{n}_{k}\right)\left(\frac{\phi^{n}_{k}}{\zeta^{n}}+\gamma^{n}_{k}-\beta^{n}_{k}\right) \\ -2\mu^{n}_{\mathrm{B},k}\left(\frac{\phi^{n}_{k}}{\zeta^{n}}+\gamma^{n}_{k}-\beta^{n}_{k}\right)+\left(\frac{\phi^{n}_{k}}{\zeta^{n}}+\gamma^{n}_{k}-\beta^{n}_{k}-1\right)\end{array}\right\} \tag{12d}$$

$$\frac{\partial D^{n}_{\mathrm{B},k}}{\partial \phi^{n}_{k}} = \hat{q}^{n}_{k}\left(\alpha^{n}_{k}\right)+\lambda^{n}_{\mathrm{A},k}\left(\frac{\theta^{n}_{k}}{\zeta^{n}}+\beta^{n}_{k}-\alpha^{n}_{k}\right)+\mu^{n}_{\mathrm{B},k}\left(\frac{\phi^{n}_{k}}{\zeta^{n}}+\gamma^{n}_{k}-\beta^{n}_{k}\right) \tag{13}$$

$$\frac{\partial D^{n}_{\mathrm{B},k}}{\partial \zeta^{n}} = -\frac{1}{\left(\zeta^{n}\right)^{2}}\left[\begin{array}{l} \lambda^{n}_{\mathrm{A},k}\left(\frac{2\phi^{n}_{k}}{\zeta^{n}}+\gamma^{n}_{k}-\beta^{n}_{k}\right)\theta^{n}_{k}+ \\ \left\{\hat{q}^{n}_{k}\left(\alpha^{n}_{k}\right)+\lambda^{n}_{\mathrm{A},k}\left(\beta^{n}_{k}-\alpha^{n}_{k}\right)+\mu^{n}_{\mathrm{B},k}\left(\frac{\phi^{n}_{k}}{\zeta^{n}}+\gamma^{n}_{k}-\beta^{n}_{k}\right)\right\}\phi^{n}_{k}\end{array}\right] \tag{14}$$

The discharge rate and control delay for section B are computed by Equations (10) and (11). Equations (12a) to (12d) are the derivatives of the control delay for section B with respect to the start of the effective green time, θ^{n}_{k}, according to the queuing formation patterns illustrated by adjustment factors β^{n}_{k} and γ^{n}_{k}. $D*^{n}_{\mathrm{B},k}$ is the changed control delay due to changes in the start of the effective green time for each queuing formation pattern.

In Equation (12a), the changed control delay is equal to the original control delay of section B and the derivatives of the control delay are zero, if β^{n}_{k} is zero and γ^{n}_{k} is greater than minus three; in this case, the duration of amber time is three seconds, when the number of queued vehicles has not increased since the start of the effective green time and the discharge of the queued vehicles has ended before the start of the actual amber time. The changed control delay consists of the original control delay and $\gamma*^{n}_{k} = \gamma^{n}_{k} - 1$ caused by the change in the end of the effective green time, in which the arrival rate is zero after the start of the effective green time and the discharge rate is still negative after the end of the actual green time. Equation (12b) gives the form of the derivatives of the control delay under the aforementioned traffic conditions in section B. In Equation (12c), the derivatives of the control delay are calculated using the changed queue lengths at the start of section B, derived from section A in a traffic situation in which the number of queued vehicles continues to increase after the start of the effective green time and discharge stops before the actual amber time. In Equation (12d), the derivatives of the control delay are calculated using $\gamma*^{n}_{k} = \gamma^{n}_{k} - 1$ and the changed number of queued vehicles at $\frac{\theta^{n}_{k}}{\zeta^{n}} + \beta^{n}_{k} + 1$, in which the arrival rate is still positive after the start of the effective green time and the discharge rate is still negative after the end of the actual green time.

For the duration of the effective green time, ϕ^{n}_{k}, in section B, the derivatives of the control delay follow the forms of a partial differential equation of the control delay in Equation (13). In

addition, the derivatives of the control delay for the reciprocal value of the cycle time are calculated using Equation (14), and these derivatives are used as a gradient to obtain a minimized objective function for non-linear mathematical programs.

2.3.3 *Section C*

A substantial change in the total control delay occurs in section C with respect to the group-based variables. The queuing formation patterns may be categorized into four formulations according to the value of the adjustment factors γ_k^n and δ_k^n. If the queue lengths are still decreasing after the end of the effective green time, γ_k^n is set as the number of time units during which the discharge rate is negative; otherwise, γ_k^n is set as zero for section C. γ_k^n indicates that there are residual queued vehicles after the effective green time and a general level of vehicular congestion on the *n*th cycle with the number of remaining vehicles. δ_k^n indicates the number of time slots during which there are no queued vehicles in lane *k* during the red time after the effective green time in the *n*th cycle. The inflow intensity of vehicles after the effective green time is captured by δ_k^n. The important criteria to decide the form of the derivatives of the control delay in section C are the value of the adjustment factors γ_k^n and δ_k^n, and the number of queue lengths in which the arrival rate is positive after the effective green time. The fluctuation of the control delay caused by the group-based variables is significant for the total control delay, and the change in the control delay for section C with respect to the group-based variables is given in Figure 5.

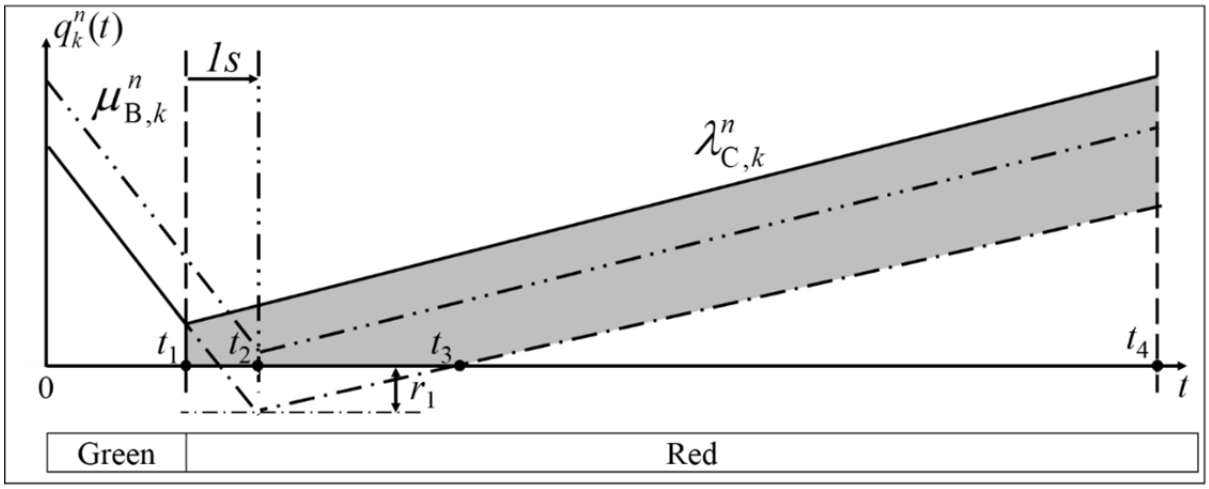

Figure 5. A change in the control delay in section C due to a minor change in the group-based variables

In Figure 5, the polygons surrounded by solid lines show the original control delay; the highlighted parts enclosed by two-dot and one dot chain lines describe the respective changes in the start and duration of the effective green time. For temporal information on the polygons of IQAs, t_1, t_2, t_3, and t_4 are $\frac{\theta_k^n + \phi_k^n}{\zeta^n} + \gamma_k^n + \delta_k^n$, $\frac{\theta_k^n + \phi_k^n}{\zeta^n} + \gamma *_k^n + \delta_k^n + 1$, $\frac{\theta_k^n + \phi_k^n}{\zeta^n} + \gamma *_k^n + \delta *_k^n + 1$, and $\frac{1}{\zeta^n}$, respectively. In addition, the gap between zero queue lengths and queue lengths in which the arrival rate begins to be positive is defined as the virtual queue lengths to be recovered, r_1. The discharge rate in lane *k* on the *n*th cycle during the effective green time, $\mu_{B,k}^n$, and the arrival rate in lane *k* on the *n*th

cycle during the red time after the effective green time, $\lambda_{C,k}^{n}$, remain unchanged by changes in the group-based variables, whereas the adjustment factors, γ_k^n and δ_k^n, can be influenced by minor changes in the group-based variables according to the temporal and spatial conditions of the queued vehicles in section C.

For changes in the start of the effective green time, the queue lengths at $\frac{\theta_k^n + \phi_k^n}{\zeta^n} + \gamma_k^n + \delta_k^n$ and $\frac{\theta_k^n + \phi_k^n}{\zeta^n} + \gamma^{*n}_k + \delta_k^n + 1$ are calculated by Equations (12a) to (12d) for section B, if δ_k^n is not negative. Moreover, the duration for recovering virtual queue lengths, r_1, replaces γ_k^n and δ_k^n to γ^{*n}_k and δ^{*n}_k, respectively, according to the traffic flow conditions for section C in subsequent equations. The queue lengths at $\frac{\theta_k^n + \phi_k^n}{\zeta^n} + \gamma^{*n}_k + \delta^{*n}_k + 1$ substitute for $\hat{q}_k^n\left(\frac{\theta_k^n + \phi_k^n}{\zeta^n} + \gamma_k^n + \delta_k^n\right)$ to calculate the changed control delay in section C. $\hat{q}_k^n\left(\frac{1}{\zeta^n}\right)$ is newly defined to reflect the changed queue lengths at the inflection point and the changed adjustment factors. Accordingly, the changed control delay is calculated based on the changed temporal and spatial information of queue lengths for section C.

For a change in the effective green-time duration, the conditions to define the new adjustment factors and queue lengths at an inflection point are similar to those for the start of the effective green time. The queue lengths at $\frac{\theta_k^n + \phi_k^n}{\zeta^n} + \gamma^{*n}_k + \delta_k^n + 1$ follow those calculated by Equation (13), if δ_k^n is set as zero. The derivatives of the control delay for the reciprocal value of the cycle time follow the form of a partial differential equation of the control delay. The conditions and formulations to compute the derivatives of the control delay with respect to the group-based variables for section C are given in the following equations derived from Equations (15) and (16).

$$\lambda_{C,k}^{n} = \frac{\hat{q}_k^n\left(\frac{1}{\zeta^n}\right) - \hat{q}_k^n\left(\frac{\theta_k^n + \phi_k^n}{\zeta^n} + \gamma_k^n + \delta_k^n\right)}{\frac{1}{\zeta^n} - \frac{\theta_k^n + \phi_k^n}{\zeta^n} - \gamma_k^n - \delta_k^n} \tag{15}$$

$$D_{C,k}^{n} = \frac{1}{2}\left\{2\hat{q}_k^n\left(\frac{1}{\zeta^n}\right) - \lambda_{C,k}^{n}\left(\frac{1}{\zeta^n} - \frac{\theta_k^n + \phi_k^n}{\zeta^n} - \gamma - \delta_k^n\right)\right\}\left(\frac{1}{\zeta^n} - \frac{\theta_k^n + \phi_k^n}{\zeta^n} - \gamma - \delta_k^n\right) \tag{16}$$

If $\beta_k^n = 0$, $\gamma_k^n \geq 0$, and $\delta_k^n = 0$,

$$D_{\mathrm{C},k}^{n}=\frac{1}{2}\left\{\begin{array}{l}2\hat{q}_{k}^{n}\left(\alpha_{k}^{n}\right)+2\lambda_{\mathrm{A},k}^{n}\left(\dfrac{\theta_{k}^{n}}{\zeta^{n}}+\beta_{k}^{n}-\alpha_{k}^{n}\right)\\+2\mu_{\mathrm{B},k}^{n}\left(\dfrac{\phi_{k}^{n}}{\zeta^{n}}+\gamma_{k}^{n}-\beta_{k}^{n}\right)\\+\lambda_{\mathrm{C},k}^{n}\left(\dfrac{1}{\zeta^{n}}-\dfrac{\theta_{k}^{n}+\phi_{k}^{n}}{\zeta^{n}}-\gamma_{k}^{n}-\delta_{k}^{n}\right)\end{array}\right\}\left(\frac{1}{\zeta^{n}}-\frac{\theta_{k}^{n}+\phi_{k}^{n}}{\zeta^{n}}-\gamma_{k}^{n}-\delta_{k}^{n}\right)$$

$$D*_{\mathrm{C},k}^{n}=\frac{1}{2}\left\{\begin{array}{l}2\hat{q}_{k}^{n}\left(\alpha_{k}^{n}\right)+2\lambda_{\mathrm{A},k}^{n}\left(\dfrac{\theta_{k}^{n}}{\zeta^{n}}+\beta_{k}^{n}-\alpha_{k}^{n}\right)\\+2\mu_{\mathrm{B},k}^{n}\left(\dfrac{\phi_{k}^{n}}{\zeta^{n}}+\gamma_{k}^{n}-\beta_{k}^{n}\right)\\+\lambda_{\mathrm{C},k}^{n}\left(\dfrac{1}{\zeta^{n}}-\dfrac{\theta_{k}^{n}+\phi_{k}^{n}}{\zeta^{n}}-\gamma_{k}^{n}-\delta_{k}^{n}-1\right)\end{array}\right\}\left(\frac{1}{\zeta^{n}}-\frac{\theta_{k}^{n}+\phi_{k}^{n}}{\zeta^{n}}-\gamma_{k}^{n}-\delta_{k}^{n}-1\right)$$

$$\frac{\partial D_{\mathrm{C},k}^{n}}{\partial\theta_{k}^{n}}=D*_{\mathrm{C},k}^{n}-D_{\mathrm{C},k}^{n}=0.5-\left\{\begin{array}{l}\hat{q}_{k}^{n}\left(\alpha_{k}^{n}\right)+\lambda_{\mathrm{A},k}^{n}\left(\dfrac{\theta_{k}^{n}}{\zeta^{n}}+\beta_{k}^{n}-\alpha_{k}^{n}\right)\\+\mu_{\mathrm{B},k}^{n}\left(\dfrac{\phi_{k}^{n}}{\zeta^{n}}+\gamma_{k}^{n}-\beta_{k}^{n}\right)\\+\lambda_{\mathrm{C},k}^{n}\left(\dfrac{1}{\zeta^{n}}-\dfrac{\theta_{k}^{n}+\phi_{k}^{n}}{\zeta^{n}}-\gamma_{k}^{n}-\delta_{k}^{n}\right)\end{array}\right\} \tag{17a}$$

If $\beta_{k}^{n}>0$, $\gamma_{k}^{n}\geq 0$, and $\delta_{k}^{n}=0$,

$$D_{\mathrm{C},k}^{n}=\frac{1}{2}\left\{\begin{array}{l}2\hat{q}_{k}^{n}\left(\alpha_{k}^{n}\right)+2\lambda_{\mathrm{A},k}^{n}\left(\dfrac{\theta_{k}^{n}}{\zeta^{n}}+\beta_{k}^{n}-\alpha_{k}^{n}\right)\\+2\mu_{\mathrm{B},k}^{n}\left(\dfrac{\phi_{k}^{n}}{\zeta^{n}}+\gamma_{k}^{n}-\beta_{k}^{n}\right)\\+\lambda_{\mathrm{C},k}^{n}\left(\dfrac{1}{\zeta^{n}}-\dfrac{\theta_{k}^{n}+\phi_{k}^{n}}{\zeta^{n}}-\gamma_{k}^{n}-\delta_{k}^{n}\right)\end{array}\right\}\left(\frac{1}{\zeta^{n}}-\frac{\theta_{k}^{n}+\phi_{k}^{n}}{\zeta^{n}}-\gamma_{k}^{n}-\delta_{k}^{n}\right)$$

$$D*_{\mathrm{C},k}^{n}=\frac{1}{2}\left[\begin{array}{l}2\hat{q}_{k}^{n}\left(\alpha_{k}^{n}\right)+2\left\{\lambda_{\mathrm{A},k}^{n}\left(\dfrac{\theta_{k}^{n}}{\zeta^{n}}+\beta_{k}^{n}-\alpha_{k}^{n}\right)+0.5\right\}\\+2\mu_{\mathrm{B},k}^{n}\left(\dfrac{\phi_{k}^{n}}{\zeta^{n}}+\gamma_{k}^{n}-\beta_{k}^{n}\right)\\+\lambda_{\mathrm{C},k}^{n}\left(\dfrac{1}{\zeta^{n}}-\dfrac{\theta_{k}^{n}+\phi_{k}^{n}}{\zeta^{n}}-\gamma_{k}^{n}-\delta_{k}^{n}-1\right)\end{array}\right]\left(\frac{1}{\zeta^{n}}-\frac{\theta_{k}^{n}+\phi_{k}^{n}}{\zeta^{n}}-\gamma_{k}^{n}-\delta_{k}^{n}-1\right)$$

$$\frac{\partial D_{\mathrm{C},k}^{n}}{\partial \theta_{k}^{n}}=\frac{1}{2}\left(\frac{1}{\zeta^{n}}-\frac{\theta_{k}^{n}+\phi_{k}^{n}}{\zeta^{n}}-\gamma_{k}^{n}-\delta_{k}^{n}+\lambda_{\mathrm{C},k}^{n}-1\right)-\hat{q}_{k}^{n}\left(\alpha_{k}^{n}\right)-\lambda_{\mathrm{A},k}^{n}\left(\frac{\theta_{k}^{n}}{\zeta^{n}}+\beta_{k}^{n}-\alpha_{k}^{n}\right)$$
$$-\mu_{\mathrm{B},k}^{n}\left(\frac{\phi_{k}^{n}}{\zeta^{n}}+\gamma_{k}^{n}-\beta_{k}^{n}\right)-\lambda_{\mathrm{C},k}^{n}\left(\frac{1}{\zeta^{n}}-\frac{\theta_{k}^{n}+\phi_{k}^{n}}{\zeta^{n}}-\gamma_{k}^{n}-\delta_{k}^{n}\right) \quad (17b)$$

The arrival rate and control delay for section C are calculated by Equations (15) and (16). The derivatives of the control delay at the start and for the duration of the effective green time are differently calculated according to the queuing formation patterns for section C defined by the adjustment factors, β_{k}^{n}, γ_{k}^{n}, δ_{k}^{n}, and the queue lengths at an inflection point, $q_{k}^{n}\left(\frac{\theta_{k}^{n}+\phi_{k}^{n}}{\zeta^{n}}+\gamma_{k}^{n}+\delta_{k}^{n}\right)$, $q_{k}^{n}\left(\frac{1}{\zeta^{n}}\right)$. $D*_{\mathrm{C},k}^{n}$ is the changed control delay due to changes in the start of the effective green time under each different queuing formation pattern for section C. The derivatives of the control delay with respect to the start of the effective green time are calculated in Equations (17a) to (17g). In Equations (17a) and (17b), the conditions of the queue formation patterns in Section C are identical, whereas the queue lengths for the first second of section C, which is decided by the queue lengths for the last second of section B, are different due to the value of β_{k}^{n} with δ_{k}^{n} decreased by one second. If β_{k}^{n} is set to zero and there is a residual queue after the effective green time, described by $\gamma_{k}^{n}\geq 0$ and $\delta_{k}^{n}=0$, the derivatives are computed by Equation (17a). In Equation (17b), in which the queue lengths are changed by the arrival of a vehicle arrived during additional spare time, β_{k}^{n}, is used in which β_{k}^{n} is larger than zero and the queued vehicles remain after the effective green time.

If $\gamma_{k}^{n}<0$, $\delta_{k}^{n}=0$, $q_{k}^{n}\left(\frac{\theta_{k}^{n}+\phi_{k}^{n}}{\zeta^{n}}+\gamma_{k}^{n}+\delta_{k}^{n}\right)\geq 1$, and $q_{k}^{n}\left(\frac{1}{\zeta^{n}}\right)\geq 1$,

$$D_{\mathrm{C},k}^{n}=\frac{1}{2}\left\{2\hat{q}_{k}^{n}\left(\frac{1}{\zeta^{n}}\right)-\lambda_{\mathrm{C},k}^{n}\left(\frac{1}{\zeta^{n}}-\frac{\theta_{k}^{n}+\phi_{k}^{n}}{\zeta^{n}}-\delta_{k}^{n}\right)\right\}\left(\frac{1}{\zeta^{n}}-\frac{\theta_{k}^{n}+\phi_{k}^{n}}{\zeta^{n}}-\delta_{k}^{n}\right)$$
$$D*_{\mathrm{C},k}^{n}=\frac{1}{2}\left\{2\hat{q}_{k}^{n}\left(\frac{1}{\zeta^{n}}\right)-\lambda_{\mathrm{C},k}^{n}\left(\frac{1}{\zeta^{n}}-\frac{\theta_{k}^{n}+\phi_{k}^{n}}{\zeta^{n}}-\delta_{k}^{n}-1\right)-2\right\}\left(\frac{1}{\zeta^{n}}-\frac{\theta_{k}^{n}+\phi_{k}^{n}}{\zeta^{n}}-\delta_{k}^{n}-1\right)$$
$$\frac{\partial D_{\mathrm{C},k}^{n}}{\partial \theta_{k}^{n}}=\frac{\partial D_{\mathrm{C},k}^{n}}{\partial \phi_{k}^{n}}=\left(\lambda_{\mathrm{C},k}^{n}-1\right)\left(\frac{1}{\zeta^{n}}-\frac{\theta_{k}^{n}+\phi_{k}^{n}}{\zeta^{n}}-\delta_{k}^{n}\right)-\hat{q}_{k}^{n}\left(\frac{1}{\zeta^{n}}\right)+1 \quad (17c)$$

If $\gamma_{k}^{n}<0$, $\delta_{k}^{n}=0$, $q_{k}^{n}\left(\frac{\theta_{k}^{n}+\phi_{k}^{n}}{\zeta^{n}}+\gamma_{k}^{n}+\delta_{k}^{n}\right)<1$, and $q_{k}^{n}\left(\frac{1}{\zeta^{n}}\right)\geq 1$,

$$D_{\mathrm{C},k}^{n}=\frac{1}{2}\left\{2\hat{q}_{k}^{n}\left(\frac{1}{\zeta^{n}}\right)-\lambda_{\mathrm{C},k}^{n}\left(\frac{1}{\zeta^{n}}-\frac{\theta_{k}^{n}+\phi_{k}^{n}}{\zeta^{n}}-\delta_{k}^{n}\right)\right\}\left(\frac{1}{\zeta^{n}}-\frac{\theta_{k}^{n}+\phi_{k}^{n}}{\zeta^{n}}-\delta_{k}^{n}\right)$$

$$D*^{n}_{\mathrm{C},k} = \frac{1}{2}\left\{2\hat{q}^{n}_{k}\left(\frac{1}{\zeta^{n}}\right) - \lambda^{n}_{\mathrm{C},k}\left(\frac{1}{\zeta^{n}} - \frac{\theta^{n}_{k}+\phi^{n}_{k}}{\zeta^{n}} - \delta*^{n}_{k} - 1\right) - 2\right\}\left(\frac{1}{\zeta^{n}} - \frac{\theta^{n}_{k}+\phi^{n}_{k}}{\zeta^{n}} - \delta*^{n}_{k} - 1\right)$$

$$\delta*^{n}_{k} = \frac{\left|\hat{q}^{n}_{k}\left(\frac{1}{\zeta^{n}}\right) - \lambda^{n}_{\mathrm{C},k}\left(\frac{1}{\zeta^{n}} - \frac{\theta^{n}_{k}+\phi^{n}_{k}}{\zeta^{n}} - \delta^{n}_{k}\right) - 1\right|}{\lambda^{n}_{\mathrm{C},k}} \tag{17d}$$

$$\frac{\partial D^{n}_{\mathrm{C},k}}{\partial \theta^{n}_{k}} = \frac{\partial D^{n}_{\mathrm{C},k}}{\partial \phi^{n}_{k}} = \frac{1}{2}\left\{\left(2\lambda^{n}_{\mathrm{C},k} - 1\right)\left(\frac{1}{\zeta^{n}} - \frac{\theta^{n}_{k}+\phi^{n}_{k}}{\zeta^{n}} - \delta*^{n}_{k}\right) - 2\hat{q}^{n}_{k}\left(\frac{1}{\zeta^{n}}\right) + 1\right\} \tag{17e}$$

If $\gamma^{n}_{k} < 0$, $\delta^{n}_{k} = 0$, $q^{n}_{k}\left(\frac{\theta^{n}_{k}+\phi^{n}_{k}}{\zeta^{n}} + \gamma^{n}_{k} + \delta^{n}_{k}\right) < 1$, and $q^{n}_{k}\left(\frac{1}{\zeta^{n}}\right) < 1$,

$$D^{n}_{\mathrm{C},k} = \frac{1}{2}\left\{2\hat{q}^{n}_{k}\left(\frac{1}{\zeta^{n}}\right) - \lambda^{n}_{\mathrm{C},k}\left(\frac{1}{\zeta^{n}} - \frac{\theta^{n}_{k}+\phi^{n}_{k}}{\zeta^{n}} - \delta^{n}_{k}\right)\right\}\left(\frac{1}{\zeta^{n}} - \frac{\theta^{n}_{k}+\phi^{n}_{k}}{\zeta^{n}} - \delta^{n}_{k}\right)$$

$$D*^{n}_{\mathrm{C},k} = 0$$

$$\frac{\partial D^{n}_{\mathrm{C},k}}{\partial \theta^{n}_{k}} = \frac{\partial D^{n}_{\mathrm{C},k}}{\partial \phi^{n}_{k}} = -\frac{1}{2}\left\{\begin{array}{l} 2\hat{q}^{n}_{k}\left(\frac{1}{\zeta^{n}}\right) \\ -\lambda^{n}_{\mathrm{C},k}\left(\frac{1}{\zeta^{n}} - \frac{\theta^{n}_{k}+\phi^{n}_{k}}{\zeta^{n}} - \delta^{n}_{k}\right) \end{array}\right\}\left(\frac{1}{\zeta^{n}} - \frac{\theta^{n}_{k}+\phi^{n}_{k}}{\zeta^{n}} - \delta^{n}_{k}\right) \tag{17f}$$

The derivatives of the control delay toward the start of the effective green time from Equation (17c) to Equation (17f), except to Equation (17d), remain unaffected by the existence and degree of residual queue lengths at the end of the effective green time, as described by $\gamma^{n}_{k} < 0$, whereas it is significant whether the numbers of queued vehicles at two inflection points on section C are larger than one, in which case δ^{n}_{k} is set to zero. Because the queue lengths at the initial temporal point in section C are independent of the number of queued vehicles at the last inflection point in section B, in which δ^{n}_{k} has a negative sign, the derivatives of the control delay with respect to the duration of the effective green time are the same as for the start of the effective green time. In Equation (17c), it is clear that a vehicle that arrives at the first time slot of section C can pass the intersection through the setback or extension of the effective green time from the value of δ^{n}_{k}, which is set to zero. Queue lengths reduced by one vehicle at two inflection points, the start and end of section C, are used to calculate the changed control delay for section C with δ^{n}_{k} decreased by one second. In Equation (17e), the conditions for the queue formation patterns in section C are similar to those in Equation (17c), except that the number of queued vehicles is less than one. To explain the recovery time for returning to zero queue lengths from negative queue lengths, the variable for the virtual queue lengths to be recovered, r_1, is introduced and the recovery time is computed in Equation (17d). To calculate the new adjustment factor, $\delta*^{n}_{k}$, the difference between the present queue lengths at the start time slot in section C and one vehicle, which may pass in one additional second, is divided by the arrival rate for

section C. $\lambda_{\mathrm{C},k}^{n}$ and $\delta *_{k}^{n}$ then replace the present δ_{k}^{n} in both the changed control delay and Equation (17e). In Equation (17f), the changed control delay in section C is set to zero, so that the queue lengths at two inflection points are smaller than one vehicle and the derivatives of the control delay are the original control delay with a negative sign.

If $\gamma_{k}^{n}<0$ and $\delta_{k}^{n}>0$,

$$D_{\mathrm{C},k}^{n}=\frac{1}{2}\left\{2\hat{q}_{k}^{n}\left(\frac{1}{\zeta^{n}}\right)-\lambda_{\mathrm{C},k}^{n}\left(\frac{1}{\zeta^{n}}-\frac{\theta_{k}^{n}+\phi_{k}^{n}}{\zeta^{n}}-\delta_{k}^{n}\right)\right\}\left(\frac{1}{\zeta^{n}}-\frac{\theta_{k}^{n}+\phi_{k}^{n}}{\zeta^{n}}-\delta_{k}^{n}\right)$$

$$D*_{\mathrm{C},k}^{n}=\frac{1}{2}\left\{2\hat{q}_{k}^{n}\left(\frac{1}{\zeta^{n}}\right)-\lambda_{\mathrm{C},k}^{n}\left(\frac{1}{\zeta^{n}}-\frac{\theta_{k}^{n}+\phi_{k}^{n}}{\zeta^{n}}-\delta_{k}^{n}-1\right)\right\}\left(\frac{1}{\zeta^{n}}-\frac{\theta_{k}^{n}+\phi_{k}^{n}}{\zeta^{n}}-\delta_{k}^{n}-1\right)$$

$$\frac{\partial D_{\mathrm{C},k}^{n}}{\partial\theta_{k}^{n}}=\frac{\partial D_{\mathrm{C},k}^{n}}{\partial\phi_{k}^{n}}=\frac{1}{2}\left\{2\lambda_{\mathrm{C},k}^{n}\left(\frac{1}{\zeta^{n}}-\frac{\theta_{k}^{n}+\phi_{k}^{n}}{\zeta^{n}}-\delta_{k}^{n}\right)-2\hat{q}_{k}^{n}\left(\frac{1}{\zeta^{n}}\right)-\lambda_{\mathrm{C},k}^{n}\right\} \tag{17g}$$

If $\gamma_{k}^{n}\geq 0$, and $\delta_{k}^{n}=0$,

$$D_{\mathrm{C},k}^{n}=\frac{1}{2}\left\{\begin{array}{l}2\hat{q}_{k}^{n}\left(\alpha_{k}^{n}\right)+2\lambda_{\mathrm{A},k}^{n}\left(\frac{\theta_{k}^{n}}{\zeta^{n}}+\beta_{k}^{n}-\alpha_{k}^{n}\right)\\+2\mu_{\mathrm{B},k}^{n}\left(\frac{\phi_{k}^{n}}{\zeta^{n}}+\gamma_{k}^{n}-\beta_{k}^{n}\right)\\+\lambda_{\mathrm{C},k}^{n}\left(\frac{1}{\zeta^{n}}-\frac{\theta_{k}^{n}+\phi_{k}^{n}}{\zeta^{n}}-\gamma_{k}^{n}-\delta_{k}^{n}\right)\end{array}\right\}\left(\frac{1}{\zeta^{n}}-\frac{\theta_{k}^{n}+\phi_{k}^{n}}{\zeta^{n}}-\gamma_{k}^{n}-\delta_{k}^{n}\right)$$

$$D*_{\mathrm{C},k}^{n}=\frac{1}{2}\left\{\begin{array}{l}2\hat{q}_{k}^{n}\left(\alpha_{k}^{n}\right)+2\lambda_{\mathrm{A},k}^{n}\left(\frac{\theta_{k}^{n}}{\zeta^{n}}+\beta_{k}^{n}-\alpha_{k}^{n}\right)\\+2\mu_{\mathrm{B},k}^{n}\left(\frac{\phi_{k}^{n}}{\zeta^{n}}+\gamma_{k}^{n}-\beta_{k}^{n}+1\right)\\+\lambda_{\mathrm{C},k}^{n}\left(\frac{1}{\zeta^{n}}-\frac{\theta_{k}^{n}+\phi_{k}^{n}}{\zeta^{n}}-\gamma_{k}^{n}-\delta_{k}^{n}-1\right)\end{array}\right\}\left(\frac{1}{\zeta^{n}}-\frac{\theta_{k}^{n}+\phi_{k}^{n}}{\zeta^{n}}-\gamma_{k}^{n}-\delta_{k}^{n}-1\right)$$

$$\frac{\partial D_{\mathrm{C},k}^{n}}{\partial\phi_{k}^{n}}=-\frac{1}{2}\left\{\begin{array}{l}2\hat{q}_{k}^{n}\left(\alpha_{k}^{n}\right)+2\lambda_{\mathrm{A},k}^{n}\left(\frac{\theta_{k}^{n}}{\zeta^{n}}+\beta_{k}^{n}-\alpha_{k}^{n}\right)+2\mu_{\mathrm{B},k}^{n}\left(\frac{\phi_{k}^{n}}{\zeta^{n}}+\gamma_{k}^{n}-\beta_{k}^{n}\right)\\-2\mu_{\mathrm{B},k}^{n}\left(\frac{1}{\zeta^{n}}-\frac{\theta_{k}^{n}+\phi_{k}^{n}}{\zeta^{n}}-\gamma_{k}^{n}-\delta_{k}^{n}\right)\\+\lambda_{\mathrm{C},k}^{n}\left(\frac{1}{\zeta^{n}}-\frac{\theta_{k}^{n}+\phi_{k}^{n}}{\zeta^{n}}-\gamma_{k}^{n}-\delta_{k}^{n}+1\right)+1\end{array}\right\} \tag{18}$$

$$\frac{\partial D_{\mathrm{C},k}^{n}}{\partial \zeta^{n}} = -\frac{1}{\left(\zeta^{n}\right)^{2}}\left[\begin{array}{l}\hat{q}_{k}^{n}\left(\frac{1}{\zeta^{n}}\right)\left\{1-\left(\theta_{k}^{n}+\phi_{k}^{n}\right)\right\}-\lambda_{\mathrm{C},k}^{n}\left(\frac{1}{\zeta^{n}}+\gamma_{k}^{n}+\delta_{k}^{n}\right) \\ +\lambda_{\mathrm{C},k}^{n}\left(\theta_{k}^{n}+\phi_{k}^{n}\right)\left(\frac{2}{\zeta^{n}}-\frac{\left(\theta_{k}^{n}+\phi_{k}^{n}\right)}{\zeta^{n}}+\gamma_{k}^{n}+\delta_{k}^{n}\right)\end{array}\right] \tag{19}$$

In Equation (17g), the number of time slots in which lane *k* is empty on the *n*th cycle during the red time after the effective green time, δ_k^n , is larger than zero. In addition, the queue lengths at the start of section C do not depend on the number of queued vehicles at the end of section B, where the number of time slots in which there are no queued vehicles in lane *k* on the *n*th cycle during the effective green time, γ_k^n , is smaller than zero. The derivatives of the control delay with respect to the start and duration of the effective green time are identical for these conditions of queuing formation patterns and are only affected by the change in the control delay caused by a one-second decrease in δ_k^n .

For the duration of the effective green time, ϕ_k^n , in section C, the derivatives of the control delay are computed in Equation (18) under the traffic conditions for θ_k^n in Equations (17a) and (17b) except for the value of β_k^n . The changed control delay considers both the one-second increase in the duration of the effective green time and the one-second decrease in the adjustment factor, δ_k^n . In addition, the derivatives of the control delay for the reciprocal value of the cycle time are calculated in Equation (19).

3. COMPARISON WITH NUMERICAL DIFFERENTIATION

To demonstrate the effectiveness of the developed equations for the derivatives of the control delay with respect to group-based variables, the results from these equations were compared with those from numerical differentiation using a typical directional three-lane, four-phase approach at an isolated intersection in VISSIM. A four-phase signalized intersection with a cycle length of 60 s was created. The green signal duration for each phase was 10 s, with an inter-green time of 5 s. A four-phase signalized intersection with control algorithms was created based on the COM interface. For numerical differentiation, the corresponding group-based variables in a particular signal group were changed by the unit time and the control delay was based on the aggregated observed queue lengths for each cycle extracted from the trajectories in VISSIM. The geometric layout of the simulated intersection is presented in Figure 6.

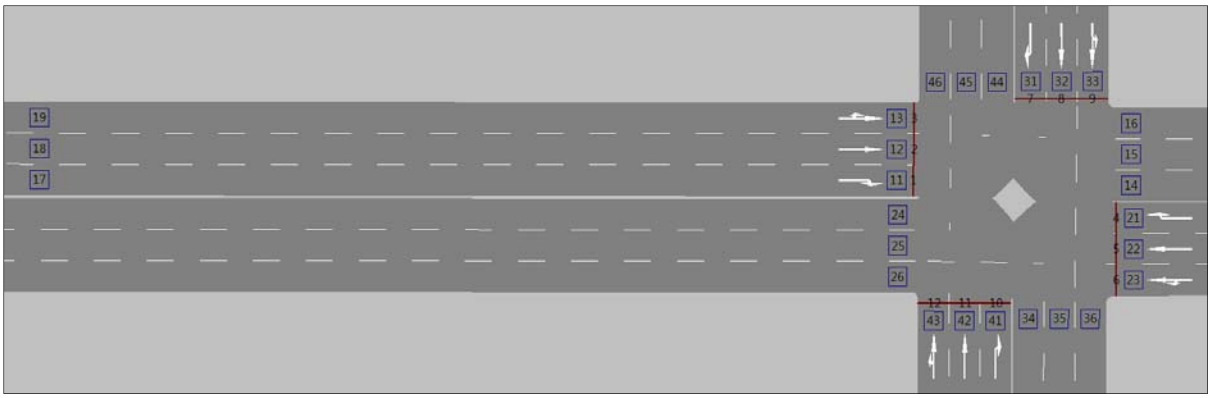

Figure 6. Geometric layout of a simulated junction in VISSIM

The simulation period was 300 s, the simulation resolution was 1 s, and the first 240 s were used as warm-up and the last cycle was used to calculate both the numerical differentiations and derivatives by means of the proposed methods. Two-hundred and seventeen simulation runs were performed with different random seeds for each set of group-based variables. Ten levels of traffic volume (degrees of saturation) from 100 (0.11) to 1000 (1.14) vph were set to illustrate the robustness and effectiveness of the proposed method. The scatter plots for comparison between numerical differentiation and the proposed methods for the derivatives of the control delay toward the start of the effective green time are illustrated in Figure 7.

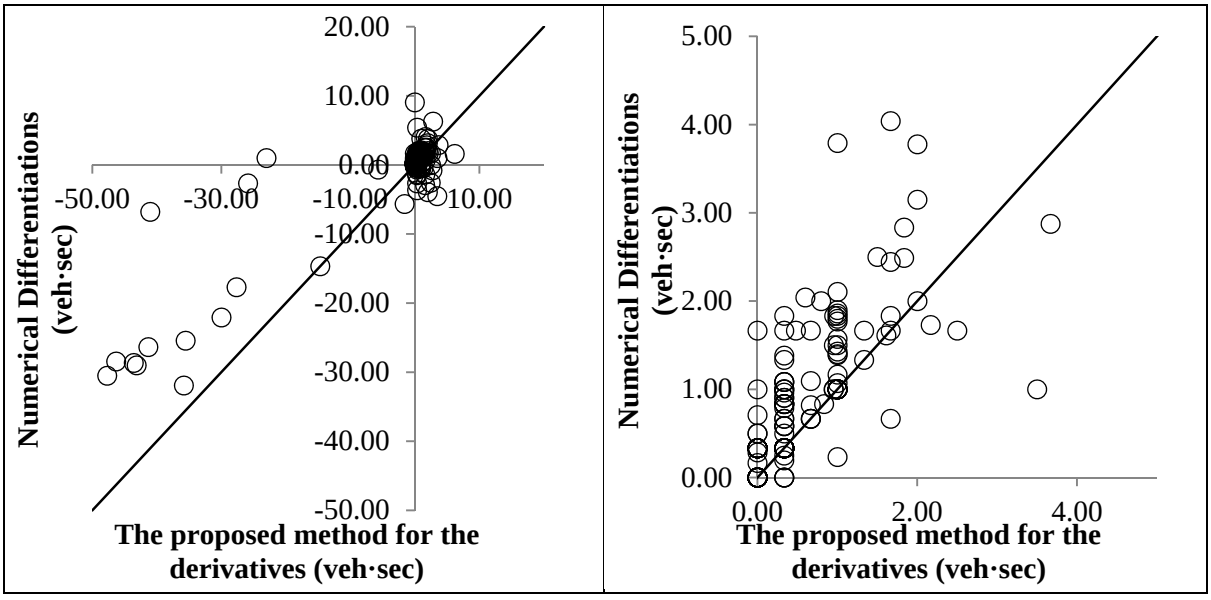

(a) Plots on a large scale (b) Plots on a small scale

Figure 7. Scatter plot of derivatives of the control delay with respect to θ_k^n

In Figure 7, the proposed methods for the derivatives of the control delay clearly perform well with numerical differentiations for each cycle. The change in the control delay due to unit changes in θ_k^n computed by the proposed equations has a linear relationship with the numerical differentiation, except for some outliers. The proposed methods capture the large amount of numerical differentiations at high levels of congestion, and the very small amount at low levels of congestion. Comparing the derivatives of the control delay and numerical differentiations shows that the proposed methods are effective and robust under diverse traffic conditions in creating derivatives of the control delay with respect to the start of the effective green time. For the duration of the effective green time,

the same simulation plan was used, and the scatter plots comparing numerical differentiations and the proposed methods for the derivatives of the control delay are illustrated in Figure 8.

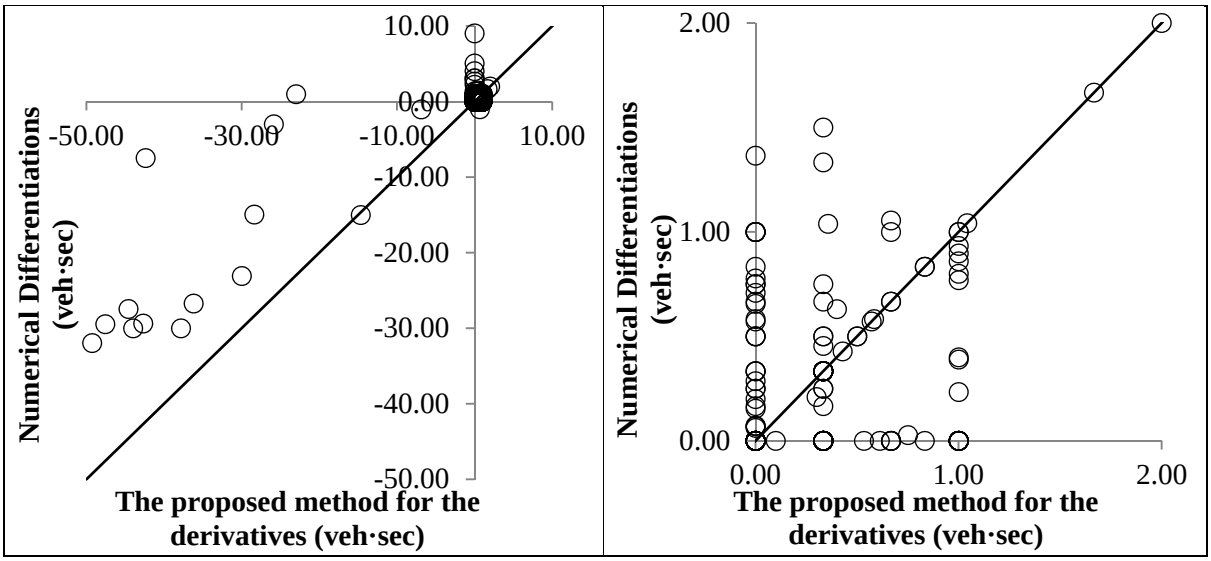

(a) Plots on a large scale (b) Plots on a small scale

Figure 8. Scatter plot of derivatives of the control delay with respect to ϕ_k^n

Figure 8 shows that the derivatives of the control delay computed by the proposed methods perform well in numerical differentiations for each cycle. Fluctuations in the control delay induced by minor changes in the corresponding group-based variables agree well with the numerical differentiation, with the exception of some outliers. The proposed methods explain not only the large changes in numerical differentiations at high levels of congestion, but also the very small fluctuations at low levels of congestion. A comparison between the derivatives of the control delay and the numerical differentiations verifies the effectiveness and robustness of the proposed methods under diverse traffic conditions for developing derivatives of the control delay with respect to the duration of the effective green time.

At first glance, the numerical results seemed worse than those of previous studies of derivatives, as we conduct a cycle-by-cycle comparison of the results of the proposed derivatives and numerical differentiations, rather than a comparison over long periods with steady-state traffic conditions. Each point shows the relationship between the results of the proposed methods and numerical differentiations for a single 60-s cycle; in other words, veh·sec is the unit in the scatter plots, not veh·hr. This means that the proposed methods capture the behavioral tendencies of a single vehicle as the control delay derived from the changes in a specific group-based variable. Accordingly, we propose using the equations of the derivatives and these simplifying procedures based on the temporal and spatial data describing the polygons in IQAs to develop a relatively simple gradient of a group-based optimization procedure with the objective function and constraints, in non-linear mathematical problems, which are solved to find the optimum cycle structure for scores of seconds in every cycle. Moreover, the RMSE values are 4.86 veh·sec and 5.20 veh·sec for the control delay with respect to start time and duration of the green phase, respectively. These results indicate that the proposed methods for approximating the derivatives of group-based variables can accurately estimate the changes in the control delay caused by the changes in each specific group-based variable on an individual lane cycle-by-cycle.

4. CONCLUSIONS

In this study, approximations for derivatives of the control delay with respect to group-based variables have been proposed for each signal group in each cycle. The key challenges were to create the formulations of the derivatives for the lane-based control delay in each cycle according to the queuing formation pattern and to identify vehicular arrivals and departures occurring in the extended or setback time duration. Temporal and spatial information on real-time queue lengths in individual lanes were collected using the estimation method for lane-based queue lengths in real time. Polygons of IQAs were used to formulate the control delay for individual lanes during each cycle on the basis of the queue lengths estimated in the previous step. Moreover, the group-based variables, including the start and the duration of the effective green time and the cycle time of each cycle, were extracted from the given signal plan and applied to formulations of the lane-based control delay. Adjustment factors were created to identify the characteristics of the queuing formation patterns for each section of each cycle. The mathematical framework for the derivatives of the control delay on sections A, B, and C was used to categorize them into groups of queuing formations defined by adjustment factors and queue lengths at an inflection point.

The proposed methods are major extensions of the method in Wong (1995), which is derived from the performance index in TRANSYT. The new methods make the following three novel contributions: 1) real-time approximate expressions of derivatives that change cycle-by-cycle according to changing queuing formation patterns, 2) mathematical frameworks for derivatives of individual lanes, and 3) dynamically adapted mathematical frameworks for the most appropriate derivatives of the control delay of group-based variables for individual lanes for each cycle.

The first contribution improves the temporal data, as the analysis time for the current real-time approximation methods is about 60 s, which is not sufficient for calculating the robust values of traffic intensities that are needed to develop the approximate expressions for derivatives in Wong (1995). The methods in Wong (1995) are suitable for estimating the average derivatives in steady-state conditions that involve no large statistical fluctuations. The current approach to the development of derivatives is not suitable for estimating the derivatives cycle-by-cycle, due to the lack of temporal and spatial data on queue lengths at the second-by-second micro level. We think that this limitation of Wong's approximate expressions for derivatives of the control delay gives rise to the relatively large deviations in cycle-by-cycle delay estimations. To overcome this disadvantage, we use the detailed temporal and spatial information on queue lengths, as estimated by the models proposed by Lee et al. (2015a) and Lee and Wong (2017), to develop a real-time group-based approach to the derivatives of the control delay for each lane, for every single cycle, with adjustment factors.

The second contribution of the proposed methods improves the spatial data, as Wong's method (1995) is unable to consider lane-changing behavior for lane-based queue lengths or the transient fluctuations of traffic flows at the micro level (second-by-second and cycle-by-cycle). The average traffic intensities, including capacity and saturation flows, the effective green times, and the cycle times, are only considered by Wong as means to approximate the derivatives of the performance index in TRANSYT. Consequently, Wong's equations are not appropriate for estimating the real-time derivatives of the control delay in each lane and in each cycle, although they do show excellent performance in steady-state traffic conditions over a long analysis period. In the submitted manuscript, we develop approximate expressions for the derivatives of the control delay model. We estimate the derivatives of the control delay on individual lanes for every single cycle under all traffic flow conditions.

For the third contribution, the dynamic adapted mathematical frameworks, we formulate the lane-based control delay in every cycle as a combination of simple polygons in IQAs, which are defined by queue lengths at inflection points, adjustment factors, and group-based variables. These are similar to the parameters and variables used in the optimization process, and here they are used to develop an inexpensive computational mathematical framework to perform a cycle-by-cycle optimization process using the most up-to-date traffic information in real time. In addition, the temporal and spatial data describing the polygons in IQAs are used to define the equations of the derivatives. These simplifying procedures are necessary to develop a relatively simple gradient of a group-based optimization procedure with the objective function and constraints, in non-linear mathematical problems, which are solved to find the optimum cycle structure for scores of seconds in every cycle.

The ultimate goal of our study is to develop a group-based adaptive traffic-signal control with a hierarchical structure consisting of tactical and local levels of signal-timing optimization. A lane-based estimation model is a prerequisite for a group-based approach to adaptive traffic-signal control. High-resolution traffic information, such as lane-based estimates, can be used as input surveillance data to achieve the same or higher levels of temporal and spatial resolution and thus take full advantage of the flexibility in group- or lane-based approaches at the tactical level and adjust the current green time according to lane-based queue lengths in real time at the local level. We comprehensively study lane-based approaches to real-time estimation methods of diverse traffic information, including lane-to-lane turning proportions in Lee et al. (2015b), lane-based queue lengths in Lee et al. (2015a), and a real-time lane-based control delay formula based on IQAs in Lee and Wong (2017). Building on our previous studies, the present manuscript proposes methods for approximating the derivatives of the lane-based control delay using the outputs of the previous studies and group-based variables. On the basis of these estimates, we devise a global proactive optimization scheme and a local reactive control policy for group-based adaptive traffic-control systems.

The derivatives of the control delay computed by the proposed methods with respect to group-based variables were compared with numerical differentiations collected through simulation. The results of the two methods were in concordance, aside from a few outliers, for the start and duration of the effective green time. The proposed methods use a simple mathematical framework to approximate the derivatives of the control delay in a cycle with group-based variables, providing a major advantage for real-time estimation and prediction. The proposed methods lay the foundations for more efficient and effective non-linear mathematical programs that optimize group-based signal plans for isolated signalized junctions, which could make use of lane-based control delay as an objective function for each cycle. Furthermore, the proposed methods will be improved to handle lane-based queue spillbacks at both upstream inflows and downstream outflows with a modified lane-based delay formulation. The derivatives calculated will play a significant role in future research into solving a non-convex function of group-based variables using a discrete directional search method in a group-based proactive mathematical optimization scheme.

Acknowledgements

The work described in this paper was jointly supported by a Research Postgraduate Studentship and grants from the University Research Committee of the University of Hong Kong (201411159005).

References

Akçelik, R., 1980. Time-dependent expressions for delay, stop rate and queue length at traffic signals. *Australian Road Research Board*, Melbourne, Australia.

Chow, A. H. F., Lo, H., 2007. Sensitivity analysis of signal control with physical queuing: Delay derivatives and an application. *Transportation Research Part B: Methodological* 41, 462-477.

Guler, S. I., Menendez, M., 2014. Analytical formulation and empirical evaluation of pre-signals for bus priority. *Transportation Research Part B: Methodological* 64, 41-53.

Heydecker, B. G., Dudgeon, I. W., 1987. Calculation of signal settings to minimise delay at a junction. In *Proceedings of the 10th International Symposium on Transportation and Traffic Theory*, MIT, July, Elsevier, New York, New York, 159-178.

Heydecker, B. G., 1992. Sequencing of traffic signals. In Griffiths, J. D. (Ed.), *Mathematics in transport and planning and control*. Clarendon Press, Oxford, U.K., 57-67.

Highway Capacity Manual, 2010. TRB, *National Research Council*, Washington D.C.

Lee, S., Wong, S. C., 2017. Group-based approach to predictive delay model based on incremental queue accumulations for adaptive traffic control systems. *Transportation Research Part B: Methodological*, vol. 98, pp. 1-20.

Lee, S., Wong, S. C., Li, Y. C., 2015a. Real-time estimation of lane-based queue lengths at isolated signalized junctions. *Transportation Research Part C: Emerging Technologies* 56, 1-17.

Lee, S., Wong, S. C., Pang, C. C. C., Choi, K., 2015b. Real-time estimation of lane-to-lane turning flows at isolated signalized junctions. *Intelligent Transportation Systems, IEEE Transactions on* 16, 1549-1558.

Lee, S., Wong, S.C., Varaiya, P., 2017a. Group-based hierarchical adaptive traffic-signal control part I: Formulation. *Transportation Research Part B: Methodological*, under review.

Lee, S., Wong, S.C., Varaiya, P., 2017b. Group-based hierarchical adaptive traffic-signal control part II: Implementation. *Transportation Research Part B: Methodological*, under review.

Lighthill M. J., Whitham G. B., 1955. On kinematic waves. I: Flood movement in long rivers. II: A theory of traffic flow on long crowded roads. In *Proceedings of the Royal Society of London A: Mathematical, Physical and Engineering Sciences*, London, U.K., A229, 281-345.

Lindley, D.V., 1952. The theory of queues with a single server, *Mathematical Proceedings of the Cambridge Philosophical Society*. Cambridge University Press, Cambridge, U.K., 277-289.

Richards, P. I., 1956. Shock waves on the highway. *Operations Research* 4, 42-51.

Saaty, T. L., 1961. *Elements of queueing theory: With application*s. McGraw-Hill, New York, New York.

Silcock, J. P., 1997. Designing signal-controlled junctions for group-based operation. *Transportation Research Part A: Policy and Practice* 31, 157-173.

Webster, F. V., 1958. Traffic signal settings, road research technical paper no. 39. *Road Research Laboratory*.

Wong, C. K., Wong, S. C., 2003a. A lane-based optimization method for minimizing delay at isolated signal-controlled junctions. *Journal of Mathematical Modelling and Algorithms* 2, 379-406.

Wong, C. K., Wong, S. C., 2003b. Lane-based optimization of signal timings for isolated junctions. *Transportation Research Part B: Methodological* 37, 63-84.

Wong, C. K., Wong, S. C., Tong, C. O., 2006. A lane-based optimization method for the multi-period analysis of isolated signal-controlled junctions. *Transportmetrica* 2, 53-85.

Wong, S. C., 1995. Derivatives of the performance index for the traffic model from TRANSYT. *Transportation Research Part B: Methodological* 29, 303-327.

Wong, S. C., 1996. Group-based optimisation of signal timings using the TRANSYT traffic model. *Transportation Research Part B: Methodological* 30, 217-244.